Universal nonequilibrium *I-V* curve near the two-channel Kondo-Luttinger quantum critical point

C.-Y. Lin,[1,2] Y.-Y. Chang,[1] C. Rylands,[3,4] N. Andrei,[3] and C.-H. Chung[1,5]

[1]*Department of Electrophysics, National Chiao-Tung University, Hsinchu 30010, Taiwan, Republic of China*
[2]*Institute of Physics, Academia Sinica, Taipei 11529, Taiwan, Republic of China*
[3]*Center for Materials Theory, Department of Physics and Astronomy, Rutgers University, Piscataway, New Jersey 08854, USA*
[4]*Joint Quantum Institute and Condensed Matter Theory Center, University of Maryland, College Park, Maryland 20742, USA*
[5]*Physics Division, National Center for Theoretical Sciences, Hsinchu 30013, Taiwan, Republic of China*

(Received 18 September 2019; revised 5 August 2020; accepted 16 August 2020; published 28 August 2020)

Over recent decades, a growing number of systems, many of them quantum critical, have been shown to exhibit non-Fermi-liquid behavior, but a full analytic understanding of such systems out of equilibrium is still lacking. In this paper, we provide a distinct example with broad applications in correlated mesoscopic systems to address this issue—a two-channel Kondo-Luttinger model where a Kondo impurity couples to two voltage-biased interacting electron leads, experimentally realizable in a dissipative quantum dot. Therein, an exotic quantum phase transition has been known to exist since the 1990s from the one-channel to two-channel Kondo ground states by enhancing electron interactions in the leads, but a controlled analytic approach to this quantum critical point has not yet been established due to the breakdown of weak-coupling perturbation theory near this strong-coupling critical point. We present a controlled method to this long-standing problem by mapping the system in the strong-coupling regime to an effective spin-boson-fermion Hamiltonian. Another type of non-Fermi-liquid quantum critical point is discovered with a distinct logarithmic-in-temperature and -voltage dependence in transport. We further obtain an analytical form for the universal differential conductance out of equilibrium near the transition. Our approach can be further generalized to study nonequilibrium physics of other strong-coupling low-dimensional non-Fermi-liquid fixed points. The relevance of our results for recent experiments is discussed.

DOI: 10.1103/PhysRevB.102.075145

I. INTRODUCTION

Over recent decades, there has been growing experimental evidence for correlated electron systems whose low-temperature thermodynamic and transport properties violate Landau's Fermi-liquid paradigm [1,2]. Such non-Fermi-liquid (NFL) behavior, ranging from heavy-fermion unconventional superconductors [3–5] to Kondo impurity quantum dot systems [6,7], often appears near a quantum phase transition (QPT) [8] as a result of competing ground states. While the equilibrium aspects of QPTs have been extensively studied, much less is known about their properties out of equilibrium. In particular, exact or analytical results are rare [9,10] despite their relevance for experiments [9–13]. The study of nonequilibrium NFL in low-dimensional systems is of wide interest not only because of its lessons to higher dimensions, but also for the large field of low-dimensional physics in mesoscopics [9,12–17], cavity electrodynamics [18], in cold atom physics [19–21], and more recently in the realization of Majorana fermions [22].

Highly tunable nanoscale quantum impurity systems offer an excellent playground to study nonequilibrium behavior near the NFL QPTs [14,23]. A typical example is the Kondo-Luttinger system, experimentally realizable in various correlated mesoscopic systems, including dissipative Kondo dot devices in carbon nanotubes [15,16] and in two-channel semiconductor quantum dot devices subject to either dissipation or electron interactions in the leads [7]. The model consists of a spin-$1/2$ Kondo impurity coupled to two Luttinger liquid wires (left L and right R) via interlead and intralead couplings, J_{LR} and $J_{LL/RR}$, involving screening of the impurity spin by the conduction electrons of both leads and of one lead, respectively. In each wire the electrons interact repulsively, their effective interaction given by a Luttinger parameter $K < 1$ [see Fig. 1(a)].

The equilibrium behavior of the system is well known. In the weak-coupling limit ($J_{\alpha\alpha'} \to 0$) at a higher temperature, the repulsive electron interactions in the leads are known to suppress the J_{LR} terms in a power-law-in-T fashion, $J_{LR} \sim T^{1/2(1/K-1)}$ [24,25]. The $J_{LL/RR}$ terms are unaffected by interactions and show a typical Kondo logarithmic decrease with increasing temperature. On the other hand, as $T \to 0$, it has been predicted since the 1990s that this model undergoes an exotic QPT from the conducting one-channel Kondo (1CK) ground state to the insulating two-channel Kondo (2CK) ground state with increasing electron interaction (or decreasing K) in the wire. In the conducting 1CK ground state both J_{LR} and $J_{LL/RR}$ couplings exhibit power-law divergences as the temperature is lowered and the two leads are coupled to form a single Kondo screening channel; in the insulating 2CK ground state, the J_{LR} ($J_{LL/RR}$) coupling is T-power-law suppressed (enhanced) and the two leads independently Kondo-screen

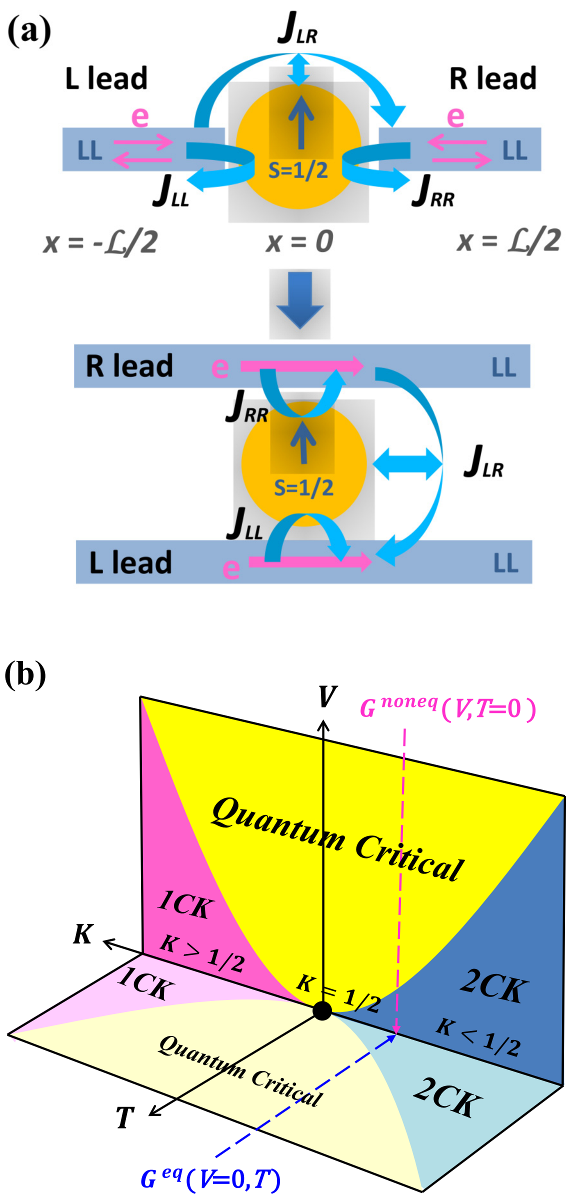

FIG. 1. (a) The original Kondo-Luttinger model (above) with two electron branches (left moving and right moving) in each of the two leads of a length $\mathcal{L}/2$ can be transformed to an equivalent chiral Kondo-Luttinger model (below) where both leads are now unfolded and extend from $-\mathcal{L}/2$ to $\mathcal{L}/2$ with only one electron branch left. (b) Schematic phase diagram of the Kondo-Luttinger model as functions of V, T, and the Luttinger parameter K.

the impurity spin [24,26]. The 1CK-2CK quantum critical point (QCP) is expected at $K = 1/2$ [see Fig. 1(b)] [24,26]. While the RG flow diagram is well understood, accessing the NFL properties of this QCP becomes challenging due to the lack of controlled theoretical approaches to physics near the strong-coupling 2CK ground state where $J_{LL/RR} \to \infty$ and the standard weak-coupling perturbation theory breaks down.

In this paper, we reexamine the Kondo-Lutinger system and establish a controlled theoretical framework to circumvent the above difficulty and study both the equilibrium and nonequilibrium transport near the 1CK-2CK QCP. This is achieved by being able to exactly map the strong-coupling problem near $K = 1/2$ onto an effective weak-coupling Hamiltonian whose nonequilibrium transport properties are then studied with the Keldysh Green's functions. By a series of transformations involving bosonizations and refermionizations detailed below, we obtain the form of the effective Hamiltonian near the 2CK fixed point in the effective weak-coupling regime. Since the current is determined by J_{LR}, we study its renormalization group (RG) flow around the QCP, which allows for a reliable study in the effective weak-coupling regime. Our RG analysis at two-loop order shows another type of NFL QCP with a distinct logarithmic-in-temperature and -voltage dependence in transport. To simplify our calculations, we work in the channel symmetric case ($J_{LL} = J_{RR}$) and near the Toulouse limit where only J_{LR} dominates. Nevertheless, our results can be extended more generally to parameter space away from the Toulouse limit. This can be done for the following reasons: (i) The operators around this limit—the transverse (xy) component of J_{LR} and the longitudinal (z) component of $J_{LL/RR}$—are all irrelevant and hence will always stay in the weak-coupling regime, and (ii) the RG flow for J_{LR} at one-loop order in this limit [see Eq. (7)] shows a negligible difference from that up to two-loop order and away from this limit [see the inset of Fig. 1(c)]. This indicates that our analytic results based on Eq. (7) are accurate and reliable enough to be extended to the parameter space away from the Toulouse limit. The universal nonlinear I-V curve of the effective model is then analytically obtained near the QCP for $K < 1/2$ and $K = 1/2$ via the Keldysh nonequilibrium Green's function formalism. Our results go beyond the equilibrium power law in transport near $K = 1/2$ given in Refs. [24,25,27] and thus offer a rare example of analytically accessible nonequilibrium transport near an impurity quantum critical point. Our analytical approach can be further generalized to study the nonequilibrium physics of other strong-coupling low-dimensional NFL fixed points.

II. THE KONDO-LUTTINGER MODEL

The Hamiltonian of our system in the presence of particle-hole symmetry reads [28,29] $H = H_0 + H_{\text{int}} + H_K + H_\mu$ with

$$H_0 = -iv_F \sum_{\alpha,\sigma} \int dx[\mathfrak{R}^\dagger_{\alpha,\sigma}(x)\partial_x \mathfrak{R}_{\alpha,\sigma}(x) - (\mathfrak{R} \leftrightarrow \mathfrak{L})],$$

$$H_{\text{int}} = \sum_{\alpha;\sigma,\sigma'} \int dx\Big[\frac{g_4}{2}[\rho_{\alpha,\sigma}(x)\rho_{\alpha,\sigma'}(x) + \overline{\rho}_{\alpha,\sigma}(x)\overline{\rho}_{\alpha,\sigma'}(x)] + g_2\rho_{\alpha,\sigma}(x)\overline{\rho}_{\alpha,\sigma'}(x)\Big],$$

$$H_\mu = \frac{eV}{2}\sum_\sigma \int dx[\rho_{L\sigma}(x) + \bar{\rho}_{L\sigma}(x) - \rho_{R\sigma}(x) - \bar{\rho}_{R\sigma}(x)],$$

$$H_K = \sum_{i;\alpha\alpha';\sigma\sigma'} J_{\alpha\alpha'}\boldsymbol{S}_i \cdot \psi^\dagger_{\alpha\sigma}(0)\frac{\boldsymbol{\tau}^i_{\sigma\sigma'}}{2}\psi_{\alpha'\sigma'}(0), \quad (1)$$

where $\alpha = L, R$, $\sigma = \uparrow, \downarrow$ are the lead and spin indices, respectively, $\boldsymbol{S}_i$ is the impurity spin, and $\boldsymbol{\tau}^i_{\sigma\sigma'}$ is the Pauli matrix with $i = x, y$, or z, and we set $\hbar = 1$. The integrations are taken from $x = -\mathcal{L}/2$ to $x = 0$ for $\alpha = L$, and from $x = 0$ to

$x = \mathcal{L}/2$ for $\alpha = R$. The electron field operator is defined as $\psi_{\alpha,\sigma}(x) = \mathfrak{R}_{\alpha,\sigma}(x) + \mathfrak{L}_{\alpha,\sigma}(x)$, with $\mathfrak{R}_{\alpha,\sigma}(x)$ [$\mathfrak{L}_{\alpha,\sigma}(x)$] being the right (left) moving electrons; the corresponding electron density operators are $\rho_{\alpha,\sigma}(x) = \mathfrak{R}^\dagger_{\alpha,\sigma}(x)\mathfrak{R}_{\alpha,\sigma}(x)$ and $\overline{\rho}_{\alpha,\sigma}(x) = \mathfrak{L}^\dagger_{\alpha,\sigma}(x)\mathfrak{L}_{\alpha,\sigma}(x)$. Here, $H_0 + H_{\rm int}$ describes the Luttinger liquid wire with H_0 being the kinetic term of free-electron leads and $H_{\rm int}$ being the electron-electron interaction in the leads, and H_μ is the bias voltage term.

We now wish to cast the Hamiltonian in a form that is convenient to study at strong coupling. To begin with, we represent H in terms of chiral boson fields through standard bosonization $\Psi_{\alpha,\sigma}(x) = \lim_{a\to 0}\frac{1}{\sqrt{2\pi a}}\eta_{\alpha,\sigma}e^{-i\phi_{\alpha,\sigma}(x)}$ with $\eta_{\alpha,\sigma}$ being the Klein factor and $\phi_{\alpha,\sigma}(x)$ being the chiral boson fields [see Fig. 1(a)] [29]. Upon bosonization, the isotropic Kondo term H_K in Eq. (1) is further divided into the transverse (xy) and longitudinal (z) components with coupling constants $J^\perp_{\alpha\alpha'}$ and $J^z_{\alpha\alpha'}$, respectively. The bosonized $J^\perp_{\alpha\alpha}$, $J^z_{\alpha\alpha}$, $J^\perp_{LR}$, J^z_{LR} terms all take different forms in boson fields [24], and $J_{LL} \neq J_{RR}$ in general. Though the Kondo couplings are isotropic in Eq. (1), $J^\perp_{\alpha\alpha'} = J^z_{\alpha\alpha'}$, the transverse and longitudinal components of $J_{\alpha\alpha'}$ after bosonization obey different RG scaling equations due to their different forms in boson fields (see below). The resulting Hamiltonian H_{cb}, expressed in terms of chiral boson fields, is then transformed into an equivalent form $H_{cb} \to U^\dagger H_{cb} U = H_{sc} + H_\mu$ with $U = e^{-iS_z\phi_s(0)}$ [24], where

$$\begin{aligned} H_{sc} &= \int_{-\frac{\mathcal{L}}{2}}^{\frac{\mathcal{L}}{2}} \frac{dx}{4\pi}\left(\sum_{\mu=c,f} v_c[\nabla\phi_\mu(x)]^2 + \sum_{\nu=s,sf} v_F[\nabla\phi_\mu(x)]^2\right) \\ &\quad + \frac{J_{LR}}{\pi a}S_x\cos\left(\frac{\phi_f}{\sqrt{K}}\right) - \frac{J^z_{LR}}{\pi a}S_z\sin\phi_{sf}\sin\left(\frac{\phi_f}{\sqrt{K}}\right) \\ &\quad + \frac{J_+}{\pi a}S_x\cos\phi_{sf} - \frac{J_-}{\pi a}S_y\sin\phi_{sf} \\ &\quad + \frac{(J^z_+ - 2\pi v_F)}{4\pi}S_z\nabla\phi_s + \frac{J^z_-}{4\pi}S_z\nabla\phi_{sf}, \\ H_\mu &= \frac{eV}{4\pi}\int_{-\frac{\mathcal{L}}{2}}^{\frac{\mathcal{L}}{2}} dx\nabla\phi_f(x). \end{aligned} \tag{2}$$

In Eq. (2), the chiral boson fields $\phi_{c/f/s/sf}$ are defined as [30]

$$\begin{aligned} \phi_c &= \sum_{\alpha=L,R}\phi_{c\alpha}/\sqrt{2}, \quad \phi_f = \sum_{\alpha=L,R}\tau^z_{\alpha,\alpha}\phi_{c\alpha}/\sqrt{2}, \\ \phi_s &= \sum_{\alpha=L,R}\phi_{s\alpha}/\sqrt{2}, \quad \phi_{sf} = \sum_{\alpha=L,R}\tau^z_{\alpha,\alpha}\phi_{s\alpha}/\sqrt{2}, \end{aligned} \tag{3}$$

with $\phi_{c\alpha} = \sum_\sigma \phi_{\alpha,\sigma}/\sqrt{2}$, $\phi_{s\alpha} = \sum_{\sigma=\uparrow}^{\downarrow}\tau^z_{\sigma,\sigma}\phi_{\alpha,\sigma}/\sqrt{2}$, and

$$\begin{aligned} J_+ &= \frac{J^\perp_{LL} + J^\perp_{RR}}{2}, \quad J_- = \frac{J^\perp_{LL} - J^\perp_{RR}}{2}, \\ J^z_+ &= \frac{J^z_{LL} + J^z_{RR}}{2}, \quad J^z_- = \frac{J^z_{LL} - J^z_{RR}}{2}. \end{aligned} \tag{4}$$

In addition, v_c is the renormalized Fermi velocity and $K \equiv \sqrt{\frac{1-g_2/(8\pi v_F+g_4)}{1+g_2/(8\pi v_F+g_4)}}$ [29].

Note that J_+, J_- become the most relevant couplings (with a scaling dimension $[J_{+/-}] = 1/2$), while J_{LR} is the leading irrelevant term for $K < 1/2$ with $[J_{LR}] = 1/2K$ and hence remains in the weak-coupling regime. The more irrelevant terms are $J^z_{+/-}$ ($[J^z_{+/-}] = 1/2K + 1$) and J^z_{LR} ($[J^z_{LR}] = 1/K + 1/2$). In the following, we discuss the model [Eq. (2)] in the channel symmetric case ($J^\perp_{LL} = J^\perp_{RR}$ and $J^z_{LL} = J^z_{RR}$), where $J_- = 0$ and $J^z_- = 0$, and near the Toulouse limit [$\delta J^z = J^z_+ - 2\pi v_F \ll O(1)$]. Also, the most relevant J_+ term is pinned at a large value, while the most irrelevant J^z_{LR} term is neglected here. As a result, only the leading irrelevant Kondo couplings J_{LR} and δJ^z terms survive.

For $K \leqslant 1/2$, by adding a decoupled bosonic bath $H_b = \frac{v_c}{4\pi}\int(\nabla\widetilde{\phi})^2dx$, we refermionize Eq. (2) near the strong-coupling 2CK fixed point and the Toulouse limit in terms of effective free fermions weakly coupled to an impurity spin and an Ohmic bosonic bath $H'_b = \frac{v_c}{4\pi}\int[\nabla\varphi(x)]^2dx$. With the following transformation [31],

$$\begin{aligned} \sqrt{\frac{1}{K}}\phi_f &= \sqrt{2}\phi'_f + \sqrt{\frac{1}{K} - 2}\varphi, \\ \sqrt{\frac{1}{K}}\widetilde{\phi} &= \sqrt{\frac{1}{K} - 2}\phi'_f - \sqrt{2}\varphi, \end{aligned} \tag{5}$$

the Hamiltonian Eq. (2) can be refermionized as $H'_{sc} + H'_\mu + H'_b = H_{sc} + H_\mu + H_b$, where

$$\begin{aligned} H'_{sc} &= \sum_{\substack{\mu=cL,cR;\\k}} v_c k\, c'^\dagger_{\mu,k}c'_{\mu,k} + \sum_{\substack{\nu=sL,sR,\\k}} v_F k\, c'^\dagger_{\nu,k}c'_{\nu,k} \\ &\quad + \frac{J_+}{\pi a}S_x\cos\phi_{sf} + \frac{J_{LR}}{\mathcal{L}}S_x\sum_{k,k'}(c'^\dagger_{cL,k}c'_{cR,k'}e^{i\sqrt{\frac{1}{K}-2}\varphi(0)} \\ &\quad + \text{H.c.}) + \frac{\delta J^z}{\sqrt{2}\mathcal{L}}S_z\sum_k(c'^\dagger_{sL,k}c'_{sL,k} + c'^\dagger_{sR,k}c'_{sR,k}), \\ H'_\mu &= eV\sqrt{K}\sum_k(c'^\dagger_{cL,k}c'_{cL,k} - c'^\dagger_{cR,k}c'_{cR,k}) \\ &\quad + eV\sqrt{1-2K}\int_{-\frac{\mathcal{L}}{2}}^{\frac{\mathcal{L}}{2}}\frac{dx}{4\pi}\nabla\varphi(x), \\ H'_b &= \frac{v_c}{4\pi}\int_{-\frac{\mathcal{L}}{2}}^{\frac{\mathcal{L}}{2}}[\nabla\varphi(x)]^2dx. \end{aligned} \tag{6}$$

Here, the k-space effective free fermions in this new basis read $c'_{\mu,k} = \frac{1}{\sqrt{\mathcal{L}}}\int_{-\frac{\mathcal{L}}{2}}^{\frac{\mathcal{L}}{2}}\Psi'_\mu(x)e^{-ikx}dx$, with $\Psi'_{cL/cR}(x) = \lim_{a\to 0}\frac{1}{\sqrt{2\pi a}}\eta_{cL/cR}e^{-i[\phi_c(x)\pm\phi'_f(x)]/\sqrt{2}}$, and $\Psi'_{sL/sR}(x) = \Psi_{sL/sR}(x) = \lim_{a\to 0}\frac{1}{\sqrt{2\pi a}}\eta_{sL/sR}e^{-i[\phi_s(x)\pm\phi_{sf}(x)]/\sqrt{2}}$. Equation (6) is an effective weak-coupling Hamiltonian (J_{LR}, $\delta J^z < 1$) near the strong-coupling ($J_+ \to \infty$) 2CK fixed point where standard perturbation theory is applicable. This Hamiltonian describes two voltage-biased free-fermion leads ($c'_{cL/cR}$) showing an interlead coupling to an impurity spin (S_x) subject to a dissipative bosonic bath, while another two free-fermion leads $c'_{sL/sR}$ couple to S_z. We will show below that this effective model of Eq. (6) gives rise to another type of the NFL QCP and distinct equilibrium and nonequilibrium transport properties near the transition.

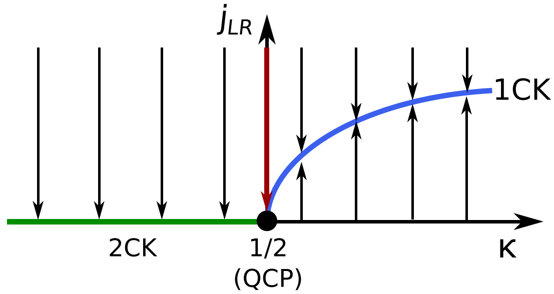

FIG. 2. The schematic diagram of the RG flow of j_{LR} with different values of K. The green (blue) line represents the line of fixed point of 2CK (1CK) The line of fixed points (blue curve) for 1CK state follows $j_{LR}^{*2} = 2(1 - \frac{1}{2K})$. $K = 1/2$ is a QCP separating the line of fixed point of 2CK and 1CK. Arrows denotes the schematic RG trajectories.

III. RG ANALYSIS OF THE EFFECTIVE HAMILTONIAN NEAR 2CK

To determine the ground state phase diagram and the nature of the phase transition in Eq. (6), we perform an RG analysis. The RG scaling equations up to one-loop order for J_{LR} and δJ^z are derived via Eq. (6) as

$$\frac{dJ_{LR}}{dl} = \left(1 - \frac{1}{2K}\right)J_{LR}, \quad \frac{d\delta J^z}{dl} = -\frac{1}{2K}\delta J^z, \tag{7}$$

where $dl = -d\Lambda/\Lambda$, with Λ being a running energy cutoff. Note that we find no quadratic contributions in Kondo couplings to Eq. (7) due to the decoupling of the fields $c_{cL/cR}$ in the J_{LR} term from $c_{sL/sR}$ in the δJ^z term. Based on Eq. (7), the J_{LR} term is irrelevant (relevant) for $K < 1/2$ ($K > 1/2$). As a result, the 1CK-2CK QCP occurs at $K = 1/2$, separating the 1CK state with $J_+ \to \infty$, $J_{LR} \to \infty$ for $K > 1/2$ from the 2CK state with $J+ \to \infty$, $J_{LR} \to 0$ for $K < 1/2$ [see Fig. 1(b)] [24]. Note that the coupling J_{LR} at the QCP is a marginal term up to one-loop RG, indicating a Fermi-liquid ground state with constant metallic conductance $G_c(V, T \to 0) = G_c^0$. However, this nature of QCP is drastically changed upon including two-loop order corrections in the RG analysis. The RG scaling equations at two-loop order read [up to cubic in coupling constants—see Appendix C (valid for $0 < K \leqslant 1/2$) and Appendix D (valid for both $K \leqslant 1/2$ and $1/2 < K < 1$) for details]

$$\begin{aligned}\frac{dj_{LR}}{dl} &= \left(1 - \frac{1}{2K}\right)j_{LR} - \frac{1}{4}(j_{LR})^3 - \frac{1}{8}(\delta j^z)^2 j_{LR},\\ \frac{d\delta j^z}{dl} &= -\frac{1}{2K}\delta j^z - \frac{1}{4}(j_{LR})^2\delta j^z - \frac{1}{8}(\delta j^z)^3\end{aligned} \tag{8}$$

with $j_{LR} = J_{LR}/2\pi v_F$ and $\delta j^z = \delta J^z/2\pi v_F$. Here, we have chosen $\hbar = 1$. The structure of Eq. (8)—the presence (absence) of linear (quadratic) in Kondo couplings—is distinct from previously studied RG scaling equations of Kondo and Anderson impurity models. Consequently, the RG flows of j_{LR} and δj^z show unique features near the QCP at $K = 1/2$. For $K > 1/2$, instead of flowing to a strong-coupling 1CK line of fixed point up to one-loop order, the j_{LR} term flows to an intermediate-coupling 1CK fixed point at $(j_{LR}^*)^2 = 2(1 - \frac{1}{2K})$ (the blue curve of Fig. 2). For $K < 1/2$, there is no new critical point appearing as the linearized RG equations near the 2CK fixed point $j_{LR}^* = (\delta j^z)^* = 0$ reduce to the same QCP via Eq. (7) (green line of Fig. 2). Note that due to decoupling of the fields $c_{cL/cR}$ in the J_{LR} term from $c_{sL/sR}$ in the J^z term, all the terms in the RG equations beyond two-loop order with even power in coupling constants vanish, and all terms with odd power in coupling constants are all more irrelevant terms. As a result, the qualitative features of our RG flow diagram in Fig. 2 survive by including higher-order terms beyond two-loop order. Moreover, the nature of the transition revealed by the RG flows in Fig. 2 represents a distinct type of quantum critical point from previously known ones (see below).

At the QCP ($K = 1/2$), the j_{LR} term is marginally irrelevant, and δj^z is strongly irrelevant; therefore, the RG equation for j_{LR} is reduced to $dj_{LR}/dl \approx (-1/4)j_{LR}^3$, leading to a logarithmic-in-Λ dependence of the marginally irrelevant j_{LR} term (see Fig. 2) [11]

$$j_{LR}(\Lambda) = \sqrt{\frac{2}{\ln(\mathcal{D}/\Lambda)}}, \tag{9}$$

with $\mathcal{D} = \Lambda_0 \exp[2/(j_{LR}^0)^2]$, Λ_0 being the ultraviolet cutoff, and $j_{LR}^0 \equiv j_{LR}(\Lambda_0)$.

For the nonequilibrium case, the running Kondo coupling $j_{LR}(\omega, \Lambda)$ in the presence of a voltage bias acquires an additional energy/frequency (ω) dependence under RG [32]. Its RG scaling equation takes the following form [11],

$$\frac{dj_{LR}(\omega)}{dl} = -\frac{1}{4}\sum_{\eta=\pm 1}\left[j_{LR}\left(\frac{\eta V}{2}\right)\right]^3 \Theta_{\omega+\eta V/2}, \tag{10}$$

where

$$\Theta(x) = \begin{cases} 1, & x > 1,\\ \frac{1}{2}, & x = 0,\\ 0, & x < 0,\end{cases} \tag{11}$$

denotes the Heaviside step function and $\Theta_{\omega+\eta V/2} = \Theta(\Lambda - |\omega + \eta V/2 + i\bar{\Gamma}|)$ with $\bar{\Gamma}$ being the decoherence rate defined as $\bar{\Gamma} = (\pi/4)\sum_{\eta,\eta'=\pm} j_{LR}^2(\omega) f(\omega - \eta V/2)[1 - f(\omega - \eta' V/2)]$. Equation (10) gives rise to the following logarithmic-in-voltage dependence of j_{LR} for $\Lambda \to 0$ and $V/T \gg 1$,

$$j_{LR}(V, \omega \to 0) \approx 2\sqrt{\frac{1}{\ln\left(\frac{2\mathcal{D}^2}{V^2}\right)} - \frac{1}{4\ln\left(\frac{\mathcal{D}}{V}\right)}}. \tag{12}$$

Via the aforementioned $j_{LR}(\Lambda)$ and $j_{LR}(V, \omega \to 0)$, the QCP at $K = 1/2$ provides an example of the NFL QCP with distinct logarithmic-in-temperature and -voltage dependence in transport (see below), therefore belonging to a different universality class.

IV. CURRENT AND CONDUCTANCE NEAR THE QCP ($K \leqslant 1/2$)

Near the QCP, the steady-state charge current, defined as the charges passing through the Kondo dot from the left to right lead per unit time, is derived from the Heisenberg

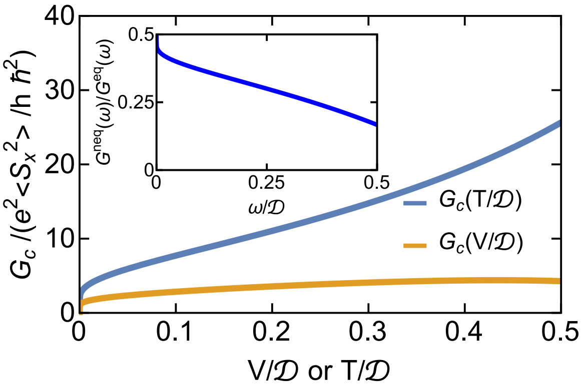

FIG. 3. The equilibrium (blue) and the nonequilibrium (orange) conductance at the QCP. The inset shows $G^{\rm neq}(\omega)/G^{\rm eq}(\omega)$ with $G^{\rm neq}(\omega) \equiv G_c(V \to \omega)$ while $G^{\rm eq}(\omega) \equiv G_c(T \to \omega)$ defined in Eqs. (16) and (20), respectively. We choose $j^0_{LR} = 0.5$.

equation of motion via Eq. (6),

$$I = -e\frac{d\langle N\rangle}{dt} = \frac{ie}{\hbar}\langle[\hat{N}, H_{sc}]\rangle$$
$$= \sqrt{K}\left(4 - \frac{1}{K}\right)\frac{e}{\hbar}\frac{J_{LR}}{\mathcal{L}}\sum_{k,k'}\mathrm{Re}\{G^<_{RL,k'k}(t,t)\}, \quad (13)$$

where $N = \sum_\sigma (N_{L\sigma} - N_{R\sigma})/2$, and $G^<_{RL,k'k}(t,t') = i\langle c'^{\dagger}_{cL,k}(t')S_x(t)c'_{cR,k'}(t)e^{i\sqrt{\frac{1}{K}-2}\varphi(t)}\rangle$ is the lesser Green's function for $c_{cL/cR,k}$.

The equilibrium transport of our model at one-loop RG for $K \leqslant 1/2$ is known [24,25]: With decreasing temperatures from the weak-coupling ($J_{\alpha\alpha'} \to 0$) fixed point at $T = \Lambda_0$, the Hamiltonian H gives a power-law-in-T suppression in the differential conductance $G(T) \sim T^{1/K-1}$ via $[J_{LR}] = (1 + 1/K)/2$, while as $T \to 0$, it shows a different power-law-in-T behavior near the QCP in the strong-coupling limit ($J_+ \to \infty$) via Eq. (7): $G(T) \sim T^{1/K-2}$ [see Fig. 1(b) and the blue dashed arrow therein]. Including contributions from the two-loop RG, the equilibrium conductance near the QCP acquires a subleading logarithmic correction,

$$G(T) \sim T^{1/K-2}/\ln\left[\frac{\mathcal{D}}{T}\right]. \quad (14)$$

Surprisingly, however, for $K = 1/2$ at the QCP, instead of the Fermi-liquid ground state with a marginal J_{LR} term up to the one-loop RG of Eq. (7), the equilibrium conductance

$$G_c(T) \equiv \left.\frac{dI|_{K=1/2}}{dV}\right|_{V\to 0} = \frac{2\sqrt{2}\pi e^2}{h}\frac{\langle S_x^2\rangle}{\hbar^2}j^2_{LR}(\Lambda \to T) \quad (15)$$

via two-loop RG displays another type of NFL QCP with logarithmic-in-temperature dependence of conductance [see $j_{LR}(\Lambda)$ and the blue curve of Fig. 3],

$$G_c(T) = \frac{e^2}{h}\frac{\langle S_x^2\rangle}{\hbar^2}\frac{4\sqrt{2}\pi}{\ln(\mathcal{D}/T)}. \quad (16)$$

Via Eq. (16), the equilibrium conductance at the QCP, $G_c(T)$, exhibits a different universal logarithmic-in-$\mathcal{D}/T$ scaling, distinct from the T-power-law behavior of a typical quantum critical point [3] and the $1/\ln^2[T/\mathcal{D}]$ in the Kosterlitz-Thouless transition of the anisotropic Kondo model [11].

A. Nonequilibrium *I-V* curve via first-order in perturbation

We now analyze the nonequilibrium transport near the QCP. Within the Keldysh nonequilibrium Green's function approach [33,34], the right-left lesser Green's function in the time domain $G^<_{RL,kk'}(t-t')$ in Eq. (13) is obtained via perturbative expansion up to first order in J_{LR}, given by [35]

$$G^<_{RL,k'k}(t-t')$$
$$= \frac{J_{LR}\langle S_x^2\rangle}{\mathcal{L}}\sum_{k''}\int_{-\infty}^{\infty}dt_1\{[g^r_{R,k'}(t-t_1)g^<_{L,k}(t_1-t')$$
$$+ g^<_{R,k'}(t-t_1)g^a_{L,k}(t_1-t')]b^<(t-t_1) + [g^r_{R,k'}(t-t_1)$$
$$+ g^<_{R,k'}(t-t_1)]g^<_{L,k}(t_1-t')b^r(t-t_1)\}, \quad (17)$$

where $g^{r/a/<}_{R/L,k}$ is the retarded/advanced/lesser component of the bare Green's functions of the effective noninteracting right/left lead, and $b^<(t-t') = -i\langle e^{-i\sqrt{\frac{1}{K}-2}\varphi(t')}e^{i\sqrt{\frac{1}{K}-2}\varphi(t)}\rangle_0$, $b^r(t-t') = -i\theta(t-t')\langle[e^{-i\sqrt{\frac{1}{K}-2}\varphi(t')}, e^{i\sqrt{\frac{1}{K}-2}\varphi(t)}]\rangle_0$ are the bare lesser and retarded bosonic correlation functions, respectively. In the thermodynamic limit, the explicit analytical form of the nonequilibrium current via Eqs. (13) reads

$$I = -\sqrt{K}\left(4 - \frac{1}{K}\right)\frac{e^2}{\hbar}V\frac{j^2_{LR}}{\Gamma(\frac{1}{K}-1)}\frac{\langle S_x^2\rangle}{\hbar^2}\left(\frac{2\pi k_BT}{D}\right)^{\frac{1}{K}-2}$$
$$\times\left|\frac{\Gamma(\frac{1}{2K} + i\frac{eV/2}{2\pi k_BT})}{\Gamma(1 + i\frac{eV/2}{2\pi k_BT})}\right|^2, \quad (18)$$

where $j_{LR} \equiv J_{LR}/2\pi\hbar v_F$, $2D$ is the bandwidth of the bosonic bath H'_b, and $\Gamma(x)$ is the gamma function. Note that both the fermionic and bosonic fields in H'_μ of Eq. (6) contribute to the current.

The conductance in the noninteracting limit ($K = 1/2$) deserves further discussions. For the $K = 1/2$ limit and setting $\langle S_x^2\rangle = \hbar^2/4$, our system in the Toulouse limit displays a fractional conductance $G = (\sqrt{2}\pi j^2_{LR}/2)(e^2/h)$ with a nonuniversal coefficient $(\sqrt{2}\pi j^2_{LR}/2)$ within the first-order in perturbation theory via Eq. (18), distinct from the quantized conductance per spin, $G = e^2/h$, as studied in Ref. [36] in the $K = 1$ limit. The origin of this "fractional" conductance comes from the nondiagonalizable (nonquadratic in fermion fields) and marginal (up to one-loop in RG) J_{LR} term [see Eq. (6)] at $K = 1/2$, leading to the conductance proportional to j^2_{LR} within the perturbative calculation. By contrast, the J_{LR} term for $K = 1$ in the Toulouse limit studied in Ref. [36] is relevant with a scaling dimension $[J_{LR}] = 1/2$. Their Hamiltonian in this case is quadratic in fermion operators and therefore can be exactly solved: The system goes to the resonant tunneling limit with $G = e^2/h$ per spin at the ground state. Note that our J_{LR} term becomes irrelevant at the two-loop RG, leading to a logarithmic correction to the J_{LR} term and to the differential conductance [refer to Eqs. (9), (12), and (20) and see below].

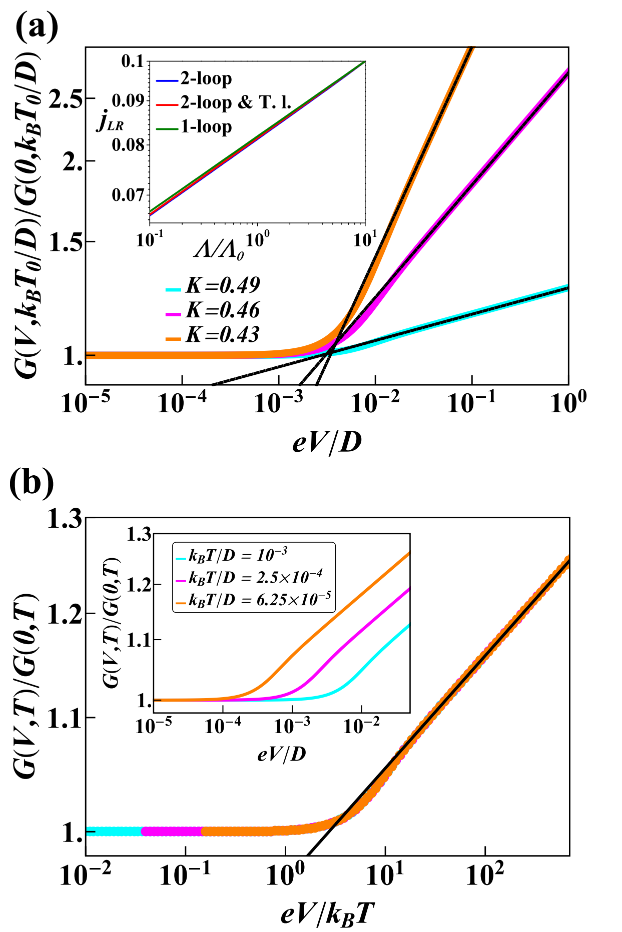

FIG. 4. (a) $G(V, k_BT_0/D)/G(0, , k_BT_0/D)$ with fixed $k_BT_0/D = 10^{-3}$, the normalized nonequilibrium differential conductance at the strong-coupling fixed point with different values of the Luttinger parameter $K \leqslant 1/2$. The black solid lines are power-law fit to $V^{1/K-2}$. Inset: RG flows for j_{LR} for $K = 0.46$ with bare coupling $j_{LR} = 0.1$ up to one-loop order (green), two-loop in the Toulouse limit (T. l., red), and two-loop away from the Toulouse limit with bare value of $\delta j^z = 0.2$ (blue). (b) Universal eV/k_BT scaling in normalized differential conductance $G(V, T)/G(0, T)$ at different values of temperature for $K = 0.49$. The inset shows nonrescaled conductances.

The analytical differential conductance $G(V, T) = dI/dV$ near the QCP for $K < 1/2$ via Eq. (18) is plotted in Figs. 4(a) and 4(b) for various values of K and temperatures. Near the QCP, the equilibrium conductance shows a power-law-in-T suppression, $G(V = 0, T) \propto T^{1/K-2}$ [27], leading to an insulating 2CK state. For $V \gg T$ and for a fixed $T = T_0$, the Γ functions in the analytic I-V curve in Eq. (18) lead to the asymptotic power-law conductance of the equilibrium form, $G(V, T_0) \sim (V/T_0)^{1/K-2}$. For $V \leqslant T$, however, $G(V, T)$ deviates from this power law and shows a universal crossover to the equilibrium value $G(0, T)$ [see the universal V/T scaling of $G(V, T)$ in Fig. 4(d)] [10]. The conductance $G(V, T)$ via Eq. (18) offers an analytical and complete universal crossover function from 2CK nonequilibrium quantum critical ($V \gg T$) to the equilibrium 2CK ($V \ll T$) limits. Our analytic crossover function in the I-V curve provides not only a qualitative but also a quantitative basis to compare with experiments. The analytic form in Eq. (7) reduces to a constant conductance for $K = 1/2$ in the wide-band ($D \to \infty$) limit [37].

B. *I-V* curve via two-loop RG

At the QCP ($K = 1/2$) (Fig. 2), the quantum critical current $I_c \equiv I(V, T)|_{K=1/2}$ via two-loop RG takes the form [see Eq. (18)]

$$I_c \approx \frac{2\sqrt{2}\pi e^2}{h} \frac{\langle S_x^2 \rangle V}{\hbar^2} \big[j_{LR}^c(\max[V, T]) \big]^2, \tag{19}$$

where $j_{LR}^c \equiv j_{LR}|_{K=1/2}$ follows from $j_{LR}(\Lambda)$ for $T \gg V$ and $j_{LR}(V, \omega \to 0)$ for $V \gg T$. The charge current therefore acquires other (logarithmic) corrections in V or T.

For $V \gg T$, we obtain an analytic form of the nonequilibrium conductance at the QCP, $G_c(V \gg T) = \frac{dI_c}{dV}$ (see the orange curve of Fig. 3),

$$G_c(V) \approx \frac{e^2}{h} \frac{8\sqrt{2}\pi \langle S_x^2 \rangle}{\hbar^2} \left[\frac{1}{\ln\left(\frac{2\mathcal{D}^2}{V^2}\right)} - \frac{1}{4\ln\left(\frac{\mathcal{D}}{V}\right)} \right]. \tag{20}$$

Note that $G_c(V \gg T)$ shows a logarithmic-in-voltage dependence, a signature of another type of NFL QCP out of equilibrium. It is a universal function of $V/\mathcal{D}$, and is distinct from its equilibrium counterpart $G_c(T, V \to 0)$ due to the nonlinear voltage dependence of the decoherence rate $\bar{\Gamma} \ll V$ (see Fig. 3), which serves as the cutoff scale for the nonequilibrium RG scheme [11,12].

For $K < 1/2$, the charge current with the inclusion of the two-loop RG correction to j_{LR} is given by $I^{\text{2-loop}} \approx \frac{I}{(j_{LR}^0)^2}[j_{LR}^c(\max[T, V])]^2$, where I is obtained via Eq. (18) within first order in perturbation theory with $j_{LR} \to j_{LR}^0$. The differential conductance $G^{\text{2-loop}} = dI^{\text{2-loop}}/dV$ therefore acquires a logarithmic correction via $j_{LR}^c(V)$, and is not a universal function of V/T.

Nevertheless, we find that $G^{\text{2-loop}}(V, T)/G_c(T, V)$ shows an approximate universal scaling in V/T for $V \gg T$ and $V \ll T$, $\frac{G^{\text{2-loop}}(V,T)}{G_c(V,T)} \approx \frac{G(V,T)}{G(0,T)} \equiv \Phi(\frac{V}{T})$, with $\Phi(V/T)$ being a universal V/T-scaling function of differential conductance via Eq. (18). Note that for $V \gg T$, contributions from $d[j_{LR}^c(V)]^2/dV$ to $G^{\text{2-loop}}(V, T)$ are negligible.

V. DISCUSSIONS AND CONCLUSIONS

First, in Refs. [15,16], the emulated Luttinger wire was realized experimentally in a spin-polarized carbon nanotube quantum dot subject to an Ohmic dissipation where the resistance R is side coupled to the dot. The effective Luttinger parameter K is related to the dimensionless dissipation strength $r \equiv Re^2/h$ via $K = 1/(1 + r)$. When the dot is symmetrically coupled to the leads, the system approaches to a quantum critical point of the 2CK type. The conductance for $V \to 0$ and $T \to 0$ reaches the unitary limit of $G(V, T) \to 2e^2/h$ in a power-law fashion, $G(V, T) \sim (V/T)^\alpha$ with $\alpha = 2/(1 + r)$. Generalizing this setup to the spinful case, a Kondo-Luttinger system equivalent to our model was proposed [27] and has been realized experimentally in a dissipative Kondo dot system with $K = 1/(1 + 2r)$ [38]. Though their Hamiltonian is somewhat different from Eq. (2), the same 1CK-2CK QPT occurs at $r = 1/2$ (or $K = 1/2$) [27]. Second, since the δj^z term is more irrelevant than j_{LR}, a finite δj^z will only lead to negligible two-loop RG corrections to j_{LR} and to the current. The RG flows for j_{LR} [see the inset of Fig. 1(c)] show a negligible difference between the results up to one-loop order in the Toulouse limit and two-loop order away from this limit. Consequently, our results can be extended to the parameter regime away from the Toulouse limit with finite δj^z. Third, the channel asymmetric J_- term is a relevant perturbation of our results, making the 2CK fixed point unstable towards the one-lead dominated 1CK fixed point. Nevertheless, channel symmetry has been achieved experimentally in an accurate and controllable manner by gate tuning in a two-channel Kondo dot device in Ref. [7] as well as for our model in Ref. [38] and for its spinless version in Refs. [15,16]. Finally, in the presence of particle-hole asymmetry, a potential scattering term $U\cos[\phi_{sf}(0)]\cos[\phi_f(0)/\sqrt{K}]$ is generated [24,25]. For $K < 1/2$, this term becomes irrelevant $[[U] = (1 + 1/K)/2]$ and can be neglected, while for $K > 1/2$, it is a relevant perturbation $[[U] = (1 + K)/2]$, and the conducting 1CK state becomes unstable towards the insulating 1CK state $[[J_{LR}] = (1 + 1/K)/2]$ with $G(T) \sim T^{1/K-1}$ as $T \to 0$.

In conclusion, we have established a framework to investigate the equilibrium and nonequilibrium transport near the strong-coupling fixed point of a Kondo-Luttinger system close to the well-known one-channel Kondo to two-channel Kondo quantum critical point at the Luttinger parameter $K = 1/2$. We discover another NFL critical point which exhibits distinct equilibrium and nonequilibrium properties.

Our work is a theoretical exploration of the nonequilibrium physics of such a non-Fermi-liquid fixed point. Its results provide an example of analytically solvable universal nonequilibrium transport near a quantum critical point in the Kondo-Luttinger system, showing a marked difference from the equilibrium properties. Our analytical approach can be further generalized to study nonequilibrium physics of other strong-coupling low-dimensional non-Fermi-liquid fixed points. Further experimental investigations in a dissipative Kondo impurity in quantum dot devices are needed to clarify our predictions.

ACKNOWLEDGMENTS

We acknowledge discussions with H. Baranger. This work is supported by the MOST Grants No. 104-2112-M-009-004-MY3 and No. 107-2112-M-009-010-MY3, the MOE-ATU 392 program, the NCTS of Taiwan, Republic of China (C.-H.C.), and NSF Grant No. DMR 1410583 (N.A.).

APPENDIX A: CHIRAL REPRESENTATION OF THE KONDO-LUTTINGER SYSTEM

In this Appendix, we will exhibit how to map the Kondo-Luttinger Hamiltonian from the original left and right moving branches basis to a chiral (one moving branch) basis in the weak tunneling limit. Although the mapping is widely used in much of the literature, for the purpose of making it more accessible to the readers, we will give a derivation with consistent notations in the main text and related to our situation directly, which demonstrate that the mapping is still valid while the charge-spin basis is used.

We start from the original Kondo-Luttinger Hamiltonian, defined as $H = H_0 + H_{\text{int}} + H_{Kf} + H_{Kb} + H_\mu$ with

$$
\begin{aligned}
H_0 &= -iv_F \sum_{\alpha;\sigma} \int [\mathfrak{R}^\dagger_{\alpha,\sigma}(x)\partial_x \mathfrak{R}_{\alpha,\sigma}(x) - (\mathfrak{R} \leftrightarrow \mathfrak{L})]dx,\\
H_{\text{int}} &= \sum_{\alpha;\sigma,\sigma'(\sigma\neq\sigma')} \int dx\Big[\frac{g_{4\parallel}}{2}[\rho^2_{\alpha,\sigma}(x) + \overline{\rho}^2_{\alpha,\sigma}(x)]\\
&\quad + \frac{g_{4\perp}}{2}[\rho_{\alpha,\sigma}(x)\rho_{\alpha,\sigma'}(x) + \overline{\rho}_{\alpha,\sigma}(x)\overline{\rho}_{\alpha,\sigma'}(x)]\\
&\quad + g_{2\parallel}\rho_{\alpha,\sigma}(x)\overline{\rho}_{\alpha,\sigma}(x) + g_{2\perp}\rho_{\alpha,\sigma}(x)\overline{\rho}_{\alpha,\sigma'}(x)\Big],\\
H_{Kf} &= \sum_{i,\sigma,\sigma'} J_{LR} S^{\text{imp}}_i \cdot \psi^\dagger_{L,\sigma}(0)\frac{\tau^i_{\sigma,\sigma'}}{2}\psi_{R,\sigma'}(0) + \text{H.c.},\\
H_{Kb} &= \sum_{i,\alpha,\sigma,\sigma'} J_{\alpha\alpha} S^{\text{imp}}_i \cdot \psi^\dagger_{\alpha,\sigma}(0)\frac{\tau^i_{\sigma,\sigma'}}{2}\psi_{\alpha,\sigma'}(0),\\
H_\mu &= \frac{eV}{2}\sum_{i,\sigma}\int [\rho_{L,\sigma}(x) + \overline{\rho}_{L,\sigma}(x) - (R \leftrightarrow L)]dx, \quad \text{(A1)}
\end{aligned}
$$

where $\alpha = L, R$, $\sigma = \uparrow, \downarrow$ are the lead and spin indices, respectively, $\tau^i_{\sigma,\sigma'}$ is the Pauli matrix, where $i = x$, y, or z, and we set $\hbar = 1$ here. In H_0 and H_{int}, the integrals are taken from $x = -\mathcal{L}/2$ to $x = 0$ for $\alpha = L$, and from $x = 0$ to $x = \mathcal{L}/2$ for $\alpha = R$. The electron field operator is defined as $\psi_{\alpha,\sigma}(x) = \mathfrak{R}_{\alpha,\sigma}(x) + \mathfrak{L}_{\alpha,\sigma}(x)$, with $\mathfrak{R}_{\alpha,\sigma}(x)$ denoting the right moving electrons and $\mathfrak{L}_{\alpha,\sigma}(x)$ the left moving ones. The electron density operators are $\rho_{\alpha,\sigma}(x) = \mathfrak{R}^\dagger_{\alpha,\sigma}(x)\mathfrak{R}_{\alpha,\sigma}(x)$ and $\overline{\rho}_{\alpha,\sigma}(x) = \mathfrak{L}^\dagger_{\alpha,\sigma}(x)\mathfrak{L}_{\alpha,\sigma}(x)$.

The charge-spin basis of the electron density operators relate to the spin-up and the spin-down basis by [28]

$$
\begin{aligned}
\rho_{c,\alpha} &= \frac{\rho_{\alpha\uparrow} + \rho_{\alpha\downarrow}}{\sqrt{2}}, \quad \overline{\rho}_{c,\alpha} = \frac{\overline{\rho}_{\alpha\uparrow} + \overline{\rho}_{\alpha\downarrow}}{\sqrt{2}},\\
\rho_{s,\alpha} &= \frac{\rho_{\alpha\uparrow} - \rho_{\alpha\downarrow}}{\sqrt{2}}, \quad \overline{\rho}_{s,\alpha} = \frac{\overline{\rho}_{\alpha\uparrow} - \overline{\rho}_{\alpha\downarrow}}{\sqrt{2}},
\end{aligned}
\quad \text{(A2)}
$$

which decouple the interaction term H_{int} into a charge sector H^c_{int} and a spin sector H^s_{int}, $H_{\text{int}} = H^c_{\text{int}} + H^s_{\text{int}}$ with

$$
\begin{aligned}
H_{\text{int}} = \sum_\alpha \int \Big[&\frac{g_4^+}{2}[\rho^2_{c,\alpha}(x)+\overline{\rho}^2_{c,\alpha}(x)] + \frac{g_4^-}{2}[\rho^2_{s,\alpha}(x)+\overline{\rho}^2_{s,\alpha}(x)]\\
&+ g_2^+\rho_{c,\alpha}(x)\overline{\rho}_{c,\alpha}(x) + g_2^-\rho_{s,\alpha}(x)\overline{\rho}_{s,\alpha}(x)\Big]dx, \quad \text{(A3)}
\end{aligned}
$$

where $g_i^+ = g_{i\parallel} + g_{i\perp}$ and $g_i^- = g_{i\parallel} - g_{i\perp}$. The interaction term H_{int} can be divided into the charge and the spin parts $H_{\text{int}} = H^c_{\text{int}} + H^s_{\text{int}}$,

$$
\begin{aligned}
H^c_{\text{int}} &= \sum_\alpha \int \Big[\frac{g_4^+}{2}\rho^2_{c,\alpha}(x) + g_2^+\rho_{c,\alpha}(x)\overline{\rho}_{c,\alpha}(x)\Big]dx,\\
H^s_{\text{int}} &= \sum_\alpha \int \Big[\frac{g_4^-}{2}\rho^2_{s,\alpha}(x) + g_2^-\rho_{s,\alpha}(x)\overline{\rho}_{s,\alpha}(x)\Big]dx. \quad \text{(A4)}
\end{aligned}
$$

In the weak tunneling limit where the electron density vanishes at the ends of the wires, the open boundary condition is imposed. A more convenient chiral field representation is used here, $\Psi_{\alpha,\sigma}(-x)=\mathfrak{R}_{\alpha,\sigma}(-x)=\mathfrak{L}_{\alpha,\sigma}(x)$, with only one species ($\mathfrak{L}$ or $\mathfrak{R}$) of electron branch or chiral fermion in each wire by unfolding the two wires from $-\mathcal{L}/2$ to $\mathcal{L}/2$ [29]. Standard bosonization is applied here: $\Psi_{\alpha,\sigma}(x)=\lim_{a\to0}\frac{1}{\sqrt{2\pi a}}\eta_{\alpha,\sigma}e^{-i\phi_{\alpha,\sigma}(x)}$. Here, $\eta_{\alpha,\sigma}$ is the Klein factor for the electron of a given species (α,σ) and $\phi_{\alpha,\sigma}(x)$ denotes the chiral boson field, which complies with the commutation relation $[\phi_{\alpha,\sigma}(x),\nabla\phi_{\alpha',\sigma'}(x')]=2\pi i\delta_{\alpha,\alpha'}\delta_{\sigma,\sigma'}\delta(x-x')$ [28,29]. Now, the Hamiltonian of the system in the chiral fermion representation reads [28]

$$
\begin{aligned}
H_0 &= -iv_F\sum_{\substack{\alpha=L,R;\\ \sigma=\uparrow,\downarrow}}\int_{-\frac{L}{2}}^{\frac{L}{2}}[\Psi^\dagger_{\alpha,\sigma}(x)\partial_x\Psi_{\alpha,\sigma}(x)]dx,\\
H_{\rm int} &= \sum_\alpha\int_{-\frac{L}{2}}^{\frac{L}{2}}\frac{1}{2}\big[g_4^+\rho^2_{c,\alpha}(x)+g_4^-\rho^2_{s,\alpha}(x)\\
&\quad+g_2^+\rho_{c,\alpha}(x)\rho_{c,\alpha}(-x)+g_2^-\rho_{s,\alpha}(x)\rho_{s,\alpha}(-x)\big]dx,\\
H_{Kf} &= \sum_{i,\sigma,\sigma'}J_{LR}S_i^{\rm imp}\cdot\Psi^\dagger_{L,\sigma}(0)\frac{\tau^i_{\sigma,\sigma'}}{2}\Psi_{R,\sigma'}(0)+\text{H.c.},\\
H_{Kb} &= \sum_{i,\alpha,\sigma,\sigma'}J_{\alpha\alpha}S_i^{\rm imp}\cdot\Psi^\dagger_{\alpha,\sigma}(0)\frac{\tau^i_{\sigma,\sigma'}}{2}\Psi_{\alpha,\sigma'}(0).
\end{aligned}\tag{A5}
$$

Upon unfolding the wires, the forms of the Kondo terms H_{Kf}, H_{Kb} and the kinetic term H_0 (with the integration taken now from $-\mathcal{L}/2$ to $\mathcal{L}/2$) are invariant. $H_{\rm int}$ can be diagonalized via the Bogoliubov rotation although there are nonlocal interactions appearing in $H_{\rm int}$ [29],

$$\rho_{c/s,\alpha}(x)\to\cosh(\varphi_{c/s})\rho_{c/s,\alpha}(x)+\sinh(\varphi_{c/s})\rho_{c/s,\alpha}(-x).\tag{A6}$$

With

$$\tanh(2\varphi_c)=\frac{-g_2^+}{8\pi v_F+g_4^+},\quad \tanh(2\varphi_s)=\frac{-g_2^-}{8\pi v_F+g_4^-},\tag{A7}$$

the rotated Hamiltonian H_0' is diagonalized, given by

$$
\begin{aligned}
H' = H_0+H_{\rm int} &= -i\int_{-\frac{L}{2}}^{\frac{L}{2}}\Bigg(v_c\sum_\alpha[\Psi^\dagger_{c,\alpha}(x)\partial_x\Psi_{c,\alpha}(x)]\\
&\quad+v_s\sum_\alpha[\Psi^\dagger_{s,\alpha}(x)\partial_x\Psi_{s,\alpha}(x)]\Bigg)dx,
\end{aligned}\tag{A8}
$$

where the renormalized Fermi velocities $v_c=(8\pi v_F+g_4^+)/\cosh(2\varphi_c)$ and $v_s=(8\pi v_F+g_4^-)/\cosh(2\varphi_s)$, and the Fermi fields in the charge-spin basis ($\Psi_{c/s,\alpha}$) and in the spin-up, spin-down basis ($\Psi_{\alpha,\uparrow/\downarrow}$) follow the same transformation as the density operators in Eq. (A2). At the same time, the bosonized form of the electron fields Ψ_μ are changed to [29]

$$\Psi_\mu(x)=\frac{\eta_\mu}{\sqrt{2\pi a}}e^{i[\frac{1}{\sqrt{K_\mu}}[\phi_\mu(x)+\phi_\mu(-x)]+\sqrt{K_\mu}[\phi_\mu(x)-\phi_\mu(-x)]]},\tag{A9}$$

where

$$
\begin{aligned}
K_{c,\alpha} &= \exp(2\varphi_c)=\sqrt{\frac{1-\frac{g_2^+}{8\pi v_F+g_4^+}}{1+\frac{g_2^+}{8\pi v_F+g_4^+}}},\\
K_{s,\alpha} &= \exp(2\varphi_s)=\sqrt{\frac{1-\frac{g_2^-}{8\pi v_F+g_4^-}}{1+\frac{g_2^-}{8\pi v_F+g_4^-}}}
\end{aligned}\tag{A10}
$$

are the charge ($K_{c,\alpha}$) and spin ($K_{s,\alpha}$) Luttinger parameters, which indicate the strength of the charge and spin interactions [29]. For a repulsive interaction, i.e., $g_{2\parallel/\perp}>0$, we have $K_{c/s}<1$, and the larger the interaction the smaller the parameter [28]. In this work, we focus on the case where only the charge interaction is involved, i.e., $K_s=1$ and $K_c=K$.

APPENDIX B: REFERMIONIZATION OF THE KONDO-LUTTINGER HAMILTONIAN FOR $K\leqslant 1/2$

In this Appendix, we give the details about the refermionization process from Eq. (2) to Eq. (6), where we refermionize the strong-coupling Kondo-Luttinger Hamiltonian in the vicinity of $K\leqslant1/2$ including the bias voltage term.

By adding an Ohmic bosonic bath $H_b=\frac{v_c}{4\pi}\int[\nabla\widetilde{\phi}(x)]^2dx$ with $\widetilde{\phi}$ being decoupled to any other field in $H_{sc}+H_\mu$ of Eq. (2), we have $[\widetilde{\phi}(x),\phi_\mu(x')]=0$ ($\mu=c,f,s,sf$). We next apply the transformation of Eq. (5) to re-fermionize the Hamiltonian of Eq. (2). Here, we choose $K\leqslant1/2$ to keep the values in the square roots of Eq. (5) real. After doing this transformation, the Hamiltonian $H_{sc}+H_\mu+H_b$ in the new basis becomes $H'_{sc}+H'_\mu+H'_b$, given by

$$
\begin{aligned}
H'_{sc} &= \int_{-\frac{\mathcal{L}}{2}}^{\frac{\mathcal{L}}{2}}\frac{dx}{4\pi}\Bigg(v_c[\nabla\phi_c(x)]^2+v_c[\nabla\phi'_f(x)]^2\\
&\quad+\sum_{v=s,sf}v_F[\nabla\phi_\mu(x)]^2\Bigg)+\frac{J_+}{\pi a}S_x\cos\phi_{sf}+\frac{\delta J_{LR}}{4\pi}S_z\nabla\phi_s\\
&\quad+\frac{J_{LR}}{\pi a}\frac{S_x}{2}(e^{i\sqrt{2}\phi'_f(0)}e^{i\sqrt{\frac{1}{K}-2}\varphi(0)}+\text{H.c.}),\\
H'_\mu &= \frac{eV}{4\pi}\int_{-\frac{\mathcal{L}}{2}}^{\frac{\mathcal{L}}{2}}dx[\sqrt{2K}\nabla\phi'_f(x)+\sqrt{1-2K}\nabla\varphi(x)],\\
H'_b &= \frac{v_c}{4\pi}\int[\nabla\varphi(x)]^2dx.
\end{aligned}\tag{B1}
$$

Define the new bosonic basis through

$$
\begin{aligned}
\phi'_{cL/cR}(x) &= \frac{\phi_c(x)\pm\phi'_f(x)}{\sqrt{2}},\\
\phi'_{sL/sR}(x) &= \phi_{sL/sR}(x)=\frac{\phi_s(x)\pm\phi_{sf}(x)}{\sqrt{2}},
\end{aligned}\tag{B2}
$$

the related new fermion operators are $\Psi'_{cL/cR}(x)=\lim_{a\to0}\frac{1}{\sqrt{2\pi a}}\eta_{cL/cR}e^{-i\phi'_{cL/cR}(x)}$ and $\Psi'_{sL/sR}(x)=\Psi_{sL/sR}(x)=\lim_{a\to0}\frac{1}{\sqrt{2\pi a}}\eta_{sL/sR}e^{-i\phi_{sL/sR}(x)}$, and the kinetic term of H'_{sc} can be refermionized as

$$\int_{-\frac{\mathcal{L}}{2}}^{\frac{\mathcal{L}}{2}} \frac{dx}{4\pi}\left(\sum_{\mu=cL,cR} v_c \Psi'^{\dagger}_{\mu}(x)\partial_x \Psi'_{\mu}(x) + \sum_{\nu=sL,sR} v_F \Psi'^{\dagger}_{\nu}(x)\partial_x \Psi'_{\nu}(x)\right)$$

via the identity $\nabla\phi(x)/4\pi = \Psi^\dagger(x)\Psi(x)$. The Kondo terms in H'_{sc} are also refermionized as

$$J_{LR}S_x\sum_{k,k'}[\Psi'^{\dagger}_{cL}(0)\Psi'_{cR}(0)e^{i\sqrt{\frac{1}{K}-2}\varphi(0)} + \text{H.c.}] + \frac{\delta J^z}{\sqrt{2}}S_z[\Psi'^{\dagger}_{sL}(0)\Psi'_{sL}(0) + \Psi'^{\dagger}_{sR}(0)\Psi'_{sR,k}(0)], \tag{B3}$$

and the bias voltage term H_μ becomes

$$H'_\mu = \frac{eV}{4\pi}\int_{-\frac{\mathcal{L}}{2}}^{\frac{\mathcal{L}}{2}} dx[\sqrt{2K}\nabla\phi'_f(x) + \sqrt{1-2K}\nabla\varphi(x)]$$
$$= eV\sqrt{K}\int_{-\frac{\mathcal{L}}{2}}^{\frac{\mathcal{L}}{2}} dx[\Psi'^{\dagger}_{cL,k}(x)\Psi'_{cL,k}(x) - \Psi'^{\dagger}_{cR,k}(x)\Psi'_{cR,k}(x)] + eV\sqrt{1-2K}\int_{-\frac{\mathcal{L}}{2}}^{\frac{\mathcal{L}}{2}} \frac{dx}{4\pi}\nabla\varphi(x).$$

Using $\Psi'_\mu(x) = \frac{1}{\sqrt{\mathcal{L}}}\sum_k c'_{\mu,k}e^{ikx}$, the refermionized Hamiltonian in a momentum representation of Eq. (6) can be readily obtained.

APPENDIX C: DERIVATION FOR RG EQUATIONS OF THE KONDO-LUTTINGER SYSTEM UP TO TWO-LOOP ORDER

In this section, we calculate the RG equations for the Kondo coupling J_{LR} and J^z to the two-loop order of Eq. (6). With the RG equations, we identify that the one-channel Kondo to two-channel Kondo quantum critical point is at the Luttinger parameter $K = 1/2$. In addition, we set $\hbar = 1$ throughout the derivation of the RG equations.

We begin with the action of Eq. (6), given by

$$S'_{sc} = \int d\tau\left(\sum_{\substack{\mu=cL,cR;\\k}} v_c k\, c'^{\dagger}_{\mu,k}c'_{\mu,k} + \sum_{\substack{\nu=sL,sR,\\k}} v_F k\, c'^{\dagger}_{\nu,k}c'_{\nu,k}\right)$$
$$- \frac{J_{LR}}{\mathcal{L}}\int d\tau S_x\sum_{k,k'}(c'^{\dagger}_{cL,k}c'_{cR,k'}e^{i\sqrt{\frac{1}{K}-2}\varphi(0)} + \text{H.c.})$$
$$- \frac{\delta J^z}{\sqrt{2}\mathcal{L}}\int d\tau S_z\sum_k(c'^{\dagger}_{sL,k}c'_{sL,k} + c'^{\dagger}_{sR,k}c'_{sR,k}),$$
$$S_b = \frac{v_c}{4\pi}\int d\tau\int[\nabla\varphi(x)]^2dx. \tag{C1}$$

To find the RG corrections to the coupling constants, we integrate out the higher-frequency modes of the fields (such as c_K or φ) in the action to obtain a low-energy effective action $S^<$ describing the low-energy behavior of the system, which is given by

$$S^<_{LR} = -\frac{J_{LR}}{\mathcal{L}}\int d\tau S_x\sum_{k,k'}(c'^{\dagger}_{cL,k}c'_{cR,k'}e^{i\sqrt{\frac{1}{K}-2}\varphi^<(0)}$$
$$\times\langle e^{i\sqrt{\frac{1}{K}-2}\varphi^>(0)}\rangle_> + \text{H.c.}), \tag{C2}$$

where $\varphi^> + \varphi^< = \varphi$, $\varphi^{>/<}$ is the higher-frequency (fast mode $\Lambda' < k < \Lambda$)/lower-frequency (slow mode $k < \Lambda'$) part of φ, and $\langle\cdots\rangle_>$ denotes the averaging with respect to only the fast mode in S_b. Thus, the first-order RG correction for J_{LR} becomes

$$J_{LR}(\Lambda') = J_{LR}(\Lambda)\left(\frac{\Lambda}{\Lambda'}\right)^{1-\frac{1}{2K}} \Rightarrow \frac{dJ_{LR}}{dl} = \left(1-\frac{1}{2K}\right)J_{LR}, \tag{C3}$$

where Λ is a running energy cutoff, $\Lambda' = \Lambda - d\Lambda$ and $dl = -d\ln|\frac{\Lambda}{\Lambda'}| = -\frac{d\Lambda}{\Lambda}$. From Ref. [39], we know that the scaling dimension of S_z is $1/2K$, which can be acquired from the correlation function of S_z, $\langle S_z(\tau)S_z(0)\rangle \propto \frac{1}{\tau^{1/K}}$. Therefore, the first-order RG corrections for δJ^z are given by

$$\frac{d\delta J^z}{dl} = -\frac{1}{2K}\delta J^z. \tag{C4}$$

Since the fermions in J_{LR} and δJ^z terms are decoupled, there are no one-loop order contributions to the RG equations of J_{LR} and δJ^z. So we go forth to compute the third-order corrections to δJ^z and J_{LR} from the third-order cumulant expansion,

$$\delta S^<_K = \frac{1}{3!}\left(\langle S^3_K\rangle_> - 3\langle S_K\rangle^2_>\langle S_K\rangle_> + 2\langle S_K\rangle^3_>\right)$$
$$= \frac{1}{3!}\langle S^3_K\rangle^c_>, \tag{C5}$$

where $\langle\cdots\rangle^c$ denotes the averaging only including the connected diagrams. It is found that there are two third-order terms, $\langle S^2_{J_{LR}}S_{\delta J^z}\rangle^c_>$ and $\langle S^3_{\delta J^z}\rangle^c_>$, which give the correction to δJ^z,

$$\begin{aligned}\delta S^{<}_{\delta J^z} =& \frac{1}{3!}\left(\left\langle S^2_{J_{LR}} S_{\delta J^z}\right\rangle_> - 3\left\langle S^2_{J_{LR}}\right\rangle_> \langle S_{\delta J^z}\rangle_> + 2\langle S_{J_{LR}}\rangle^2_> \langle S_{\delta J^z}\rangle_>\right) = \frac{1}{3!}\left\langle S^2_{J_{LR}} S_{\delta J^z}\right\rangle^c_> \\ =& -\frac{1}{3!}\frac{J^2_{LR}}{4}\frac{\delta J^z}{2}\int d\tau d\tau' d\tau'' T_\tau[S_+(\tau)S_-(\tau')S_z(\tau'')]\{\langle[\psi'^{\dagger}_{L\uparrow}(\tau)\psi'_{R\downarrow}(\tau)\psi'^{\dagger}_{R\downarrow}(\tau')\psi'_{L\uparrow}(\tau')e^{i\sqrt{1/k-1}\varphi(\tau)}e^{-i\sqrt{1/k-1}\varphi(\tau')} \\ &+ \psi'^{\dagger}_{R\uparrow}(\tau)\psi'_{L\downarrow}(\tau)\psi'^{\dagger}_{L\downarrow}(\tau')\psi'_{R\uparrow}(\tau')e^{-i\sqrt{1/k-1}\varphi(\tau)}e^{i\sqrt{1/k-1}\varphi(\tau')}][\psi'^{\dagger}_{L\uparrow}(0)\psi'_{L\uparrow}(0) - \psi'^{\dagger}_{L\downarrow}(0)\psi'_{L\downarrow}(0) \\ &+ \psi'^{\dagger}_{R\uparrow}(0)\psi'_{R\uparrow}(0) - \psi'^{\dagger}_{R\downarrow}(0)\psi'_{R\downarrow}(0)]\rangle^c_>\} \times 3!. \end{aligned} \tag{C6}$$

So the correction to δJ^z is

$$\begin{aligned}\delta(\delta J^z) =& \frac{J^2_{LR}\delta J^z}{8}\frac{1}{(\beta\mathcal{L})^2}\sum_{k;i\omega,i\omega'}\int d\tau d\tau' d\tau''\int\frac{d\omega_1 d\omega_2}{(2\pi i)^2}\left[\frac{e^{i\omega_1(\tau-\tau'')}}{\omega_1 - i\eta}\frac{e^{i\omega_2(\tau'-\tau'')}}{\omega_2 - i\eta}\right. \\ &\left.+ \frac{e^{i\omega_1(\tau''-\tau)}}{\omega_1 - i\eta}\frac{e^{i\omega_2(\tau''-\tau')}}{\omega_2 - i\eta} - \frac{e^{i\omega_1(\tau-\tau'')}}{\omega_1 - i\eta}\frac{e^{i\omega_2(\tau''-\tau')}}{\omega_2 - i\eta} - \frac{e^{i\omega_1(\tau'-\tau'')}}{\omega_1 - i\eta}\frac{e^{i\omega_2(\tau''-\tau)}}{\omega_2 - i\eta}\right] \\ &\times\left(\frac{e^{-i\omega(\tau-\tau')}}{i\omega-\varepsilon_k}\frac{e^{-i\omega'(\tau'-\tau'')}}{i\omega'-\varepsilon_k} + \frac{e^{-i\omega(\tau''-\tau)}}{i\omega-\varepsilon_k}\frac{e^{-i\omega'(\tau-\tau')}}{i\omega'-\varepsilon_k} - \frac{e^{-i\omega(\tau-\tau'')}}{i\omega-\varepsilon_k}\frac{e^{-i\omega'(\tau''-\tau')}}{i\omega'-\varepsilon_k}\right) \\ =& \frac{J^2_{LR}\delta J^z}{8}\frac{1}{(\beta\mathcal{L})^2}\sum_k\left[\frac{-f(\varepsilon_k)f(-\varepsilon_k)}{(\varepsilon_k-\eta)(\varepsilon_k+\eta)} + \frac{-f(-\varepsilon_k)f(\varepsilon_k)}{(\varepsilon_k+\eta)(\varepsilon_k-\eta)} + \frac{[f(-\varepsilon_k)]^2}{(\varepsilon_k+\eta)^2} + \frac{[f(\varepsilon_k)]^2}{(\varepsilon_k-\eta)^2}\right] \\ =& \frac{J^2_{LR}\delta J^z}{8}\frac{1}{(\beta\mathcal{L})^2}\sum_k\left[\frac{f(-\varepsilon_k)}{\varepsilon_k+\eta} - \frac{f(\varepsilon_k)}{\varepsilon_k-\eta}\right]^2 = -\frac{J^2_{LR}\delta J^z}{4(2\pi v_F)^2}dl. \end{aligned} \tag{C7}$$

Following a similar approach, the other third-order correction proportional to $(\delta J^z)^3$ is given by

$$\begin{aligned}\left\langle S^3_{\delta J^z}\right\rangle^c_> =& \frac{(\delta J^z)^3}{8}\int d\tau_1 d\tau_2 d\tau_3 T_\tau[S_z(1)S_z(2)S_z(3)]\{\langle[\psi'^{\dagger}_{L\uparrow}(1)\psi'_{L\uparrow}(1) - \psi'^{\dagger}_{L\downarrow}(1)\psi'_{L\downarrow}(1) + \psi'^{\dagger}_{R\uparrow}(1)\psi'_{\uparrow}(1) - \psi'^{\dagger}_{R\downarrow}(1)\psi'_{R\downarrow}(1)] \\ &\times[\psi'^{\dagger}_{L\uparrow}(2)\psi'_{L\uparrow}(2) - \psi'^{\dagger}_{L\downarrow}(2)\psi'_{L\downarrow}(2) + \psi'^{\dagger}_{R\uparrow}(2)\psi'_{R\uparrow}(2) - \psi'^{\dagger}_{R\downarrow}(2)\psi'_{R\downarrow}(2)] \\ &\times[\psi'^{\dagger}_{L\uparrow}(3)\psi'_{L\uparrow}(3) - \psi'^{\dagger}_{L\downarrow}(3)\psi'_{L\downarrow}(3) + \psi'^{\dagger}_{R\uparrow}(3)\psi'_{R\uparrow}(3) - \psi'^{\dagger}_{R\downarrow}(3)\psi'_{R\downarrow}(3)]\rangle^c_>\} \times 3!, \end{aligned} \tag{C8}$$

leading to

$$\begin{aligned}\delta(\delta J^z) &= \frac{1}{3!}\left(\frac{J^z}{2}\right)^3\frac{3!}{4}\int d\tau d\tau'\langle\psi'^{>}_{L\uparrow}(\tau)\psi'^{\dagger>}_{L\uparrow}(0)\rangle_>, \\ \langle\psi'^{>}_{L\uparrow}(\tau')\psi'^{\dagger>}_{L\uparrow}(0)\rangle_> &= -\frac{(\delta J^z)^3}{8(2\pi v_F)}dl. \end{aligned} \tag{C9}$$

Following a similar procedure, we can obtain the third-order corrections to J_{LR} as well. There are also two corrections to J_{LR} coming from $\langle S^2_{J^z}S_{J_{LR}}\rangle^c_>$ and $\langle S^3_{J_{LR}}\rangle^c_>$. The correction to J_{LR} from $\langle S^2_{J^z}S_{J_{LR}}\rangle^c_>$ is

$$\delta J_{LR} = -\frac{(\delta J^z)^2 J_{LR}}{8(2\pi v_F)}dl, \tag{C10}$$

and the other correction from $\langle S^3_{J_{LR}}\rangle^c_>$ is

$$\delta J_{LR} = -\frac{J^3_{LR}}{4(2\pi v_F)}dl. \tag{C11}$$

Defining the renormalized Kondo couplings $\frac{J_{LR}}{2\pi v_F} \to j_{LR}$ and $\frac{\delta J^z}{2\pi v_F} \to \delta j^z$, and collecting all the corrections of J_{LR} and δJ_z of the first to the third order, we conclude that the RG equations to the third order for J_{LR} and δJ^z, as shown in Eq. (8).

APPENDIX D: RG EQUATIONS VIA BOSONIZED HAMILTONIAN

In this Appendix, provide derivations of the RG equations via using the bosonized Kondo-Luttinger Hamiltonian of Eq. (2), which is valid for both $K \leqslant 1/2$ and $K > 1/2$.

The bosonized Kondo-Luttinger Hamiltonian takes the form

$$H = H_0 + J_{LR}S_x\cos\left(\frac{\varphi_f}{\sqrt{K}}\right) + \delta J^z S_z\partial_x\phi_s, \tag{D1}$$

where

$$H_0 = \int_{-\frac{\mathcal{L}}{2}}^{\frac{\mathcal{L}}{2}}\frac{dx}{4\pi}\left(\sum_{\mu=c,f}v_c[\nabla\phi_\mu(x)]^2 + \sum_{\nu=s,sf}v_F[\nabla\phi_\mu(x)]^2\right). \tag{D2}$$

1. RG equation for δJ^z from $J^2_{LR}\delta J^z$

The correction from the $J^2_{LR}\delta J^z$ term for δJ_z is given by

$$\begin{aligned}\delta(\delta J^z) &= -\frac{3!}{3!}\frac{1}{4}\frac{2}{4}J^2_{LR}\delta J^z\int d\tau_1 d\tau_2 d\tau_3 T_\tau[S^+(\tau_1)S^-(\tau_2)S_z(\tau_3)]\langle e^{\frac{i\phi_f(\tau_1)}{\sqrt{K}}}e^{-\frac{i\phi_f(\tau_2)}{\sqrt{K}}}\partial_{x_3}\phi_s(\tau_3)\rangle_>\\
&= -\frac{1}{8}J^2_{LR}\delta J^z\int d\tau_1 d\tau_2\langle e^{\frac{i\phi_f(\tau_1)}{\sqrt{K}}}e^{-\frac{i\phi_f(\tau_2)}{\sqrt{K}}}\rangle_> e^{\frac{i\phi_f^<(\tau_1)}{\sqrt{K}}}e^{-\frac{i\phi_f^<(\tau_2)}{\sqrt{K}}}\int d\tau_3 S_z(\tau_3)\partial_{x_3}\phi_s^<(\tau_3)\\
&= -\frac{1}{8}J^2_{LR}\delta J^z\left(\frac{\mu'}{\mu}\right)^{-2}\left(\frac{\mu'}{\mu}\right)^{1/K}\left(\frac{\mu'}{\mu}\right)^{-1/K}\left(\frac{\mu'}{\mu}\right)^{1/2K}\int d\tau_1' d\tau_2' d\tau_3' S_z'(\tau_3')\partial_{x_3}\phi_s^<(\tau_3')\\
&= -\frac{1}{8}j^2_{LR}\delta j^z\left(\frac{1}{K}\frac{d\mu'}{\mu'}\right)\int d\tau_3' S_z'(\tau_3')\partial_{x_3}\phi_s^<(\tau_3')\\
&= -\frac{1}{4}j^2_{LR}\delta j^z dl\int d\tau_3' S_z'(\tau_3')\partial_{x_3}\phi_s^<(\tau_3'),\end{aligned}\tag{D3}$$

where $j_{LR}\equiv J_{LR}(\mu'/\mu)^{-2+1/K}$ and $\delta j^z\equiv\delta J^z(\mu'/\mu)^{1/2K}$. Here, we have approximated $\ln(\mu/\mu')\approx dl$ with $dl=-d\mu/\mu$ and $d\mu\equiv\mu'-\mu$ by Taylor expansion, and $\tau\to\tau'/(\mu'/\mu)$, $x\to x'(\mu'/\mu)$, and $S_z\to S_z'(\mu'/\mu)^{1/2K}$. $J_{LR}(\Lambda')=J_{LR}(\Lambda)\langle e^{i\sqrt{-2+K^{-1}}\phi_s^>(0)}\rangle_> = (\Lambda/\Lambda')^{1-(2K)^{-1}}J_{LR}(\Lambda)$. Note that in the short-time limit $\tau\sim a\ll\mu$ (a being the lattice constant), we may get rid of the double time integrals $d\tau_1 d\tau_2$ above by introducing a short-time cutoff $\tau_0\approx a/v_f$, and absorbed it in j_{LR} via a redefinition.

2. RG equation for δJ^z from $(\delta J^z)^3$

The third-order correction for δJ^z from $(\delta J^z)^3$ is given by

$$\begin{aligned}\delta(\delta J^z) &= -\frac{3!}{3!}(\delta J^z)^3\int d\tau_1 d\tau_2 d\tau_3 T_\tau[S_z(\tau_1)S_z(\tau_2)S_z(\tau_3)]\langle\partial_x\phi_s(\tau_1)\partial_x\phi_s(\tau_2)\partial_x\phi_s(\tau_3)\rangle_>\\
&= -\frac{1}{4}(\delta J^z)^3\int d\tau^+ d\tau^-\langle\partial_x\phi_s(\tau^-)\partial_x\phi_s(0)\rangle_>\frac{1}{\tau^{1/K}}\int d\tau_3 S_z(\tau_3)\partial_x\phi_s^<(\tau_3),\end{aligned}\tag{D4}$$

where $\langle S_z(\tau)S_z(0)\rangle=\frac{1}{4\tau^{1/K}}$. Also, we may use the relation $\partial_x\phi_s=(-i/v_f)\partial_\tau\theta_s$, where ϕ_s and θ_s are conjugate variables, and $\langle\theta_s(\tau)\theta_s(0)\rangle\sim\ln(\tau)/2$. We therefore have the following relation,

$$\begin{aligned}\int d\tau^+ d\tau^-\langle\partial_x\phi_s^>(\tau^-)\partial_x\phi_s^>(0)\rangle &= \left(-v_f^{-2}\right)\int d\tau^+ d\tau^-\langle\partial_{\tau^+}\theta_s^>(0)\partial_{\tau^-}\theta_s^>(\tau^-)\rangle\\
&= \left(-v_f^{-2}\right)\int d\tau^-\partial_{\tau^-}\langle\theta_s^>(\tau^-)\theta_s^>(0)\rangle.\end{aligned}\tag{D5}$$

Combining the above relations, we obtain

$$\begin{aligned}\delta(\delta J^z) &= -\frac{1}{8}(\delta J^z)^3\ln\left[\frac{\mu}{\mu'}\right]\left(\frac{\mu'}{\mu}\right)^{1/K}\left(\frac{\mu'}{\mu}\right)^{1/2K}\int d\tau_3' S_z(\tau_3')\partial_x\phi_s^<(\tau_3')\\
&= -\frac{1}{8}(\delta j^z)^3 dl\int d\tau_3' S_z(\tau_3')\partial_x\phi_s^<(\tau_3'),\end{aligned}\tag{D6}$$

where $1/v_f^2$ is absorbed in the redefinition of δj^z. Finally, the RG equation for δj^z is given by

$$\frac{d\delta j^z}{dl}=-\frac{1}{8}(\delta j^z)^3.\tag{D7}$$

APPENDIX E: THE NONEQUILIBRIUM CURRENT FOR $K\leqslant 1/2$

In this Appendix, we supply the detailed derivations of the nonequilibrium (finite bias) charge current for the Kondo-Luttinger system [Eq. (18)] for $K\leqslant 1/2$ via the nonequilibrium Green's function technique.

The steady-state charge current, defined as the charges passing through the Kondo dot from the left to right lead per unit time, is derived from the Heisenberg equation of motion of the refermionized Hamiltonian [Eq. (6)],

$$I=-e\frac{d\langle N\rangle}{dt}=\frac{\sqrt{2}ie}{\hbar}\langle[N,H_{sc}'+H_\mu'+H_b']\rangle,\tag{E1}$$

where

$$N=\frac{N_L-N_R}{2}=\int\frac{dx}{2\pi}\nabla\phi_f(x),\tag{E2}$$

and with the transformation, Eq. (5),

$$N = \int \frac{dx}{2\pi}[\sqrt{2K}\nabla\phi'_f(x) + \sqrt{1-2K}\nabla\varphi(x)]$$
$$= \sqrt{K}\sum_k [c'^{\dagger}_{cL,k}c'_{cL,k} - c'^{\dagger}_{cR,k}c'_{cR,k}] + \int \frac{dx}{2\pi}[\sqrt{1-2K}\nabla\varphi(x)]. \tag{E3}$$

Therefore,

$$I = \frac{ie}{\hbar}\left\langle\left[N, \frac{J_{LR}}{\mathcal{L}}S_x\sum_{k,k'}(c'^{\dagger}_{cL,k}c'_{cR,k'}e^{i\sqrt{\frac{1}{K}-2}\varphi(0)} + \text{H.c.})\right]\right\rangle. \tag{E4}$$

With

$$\left\langle\left[\sqrt{K}\sum_k[c'^{\dagger}_{cL,k}c'_{cL,k} - c'^{\dagger}_{cR,k}c'_{cR,k}], S_x\sum_{k,k'}(c'^{\dagger}_{cL,k}c'_{cR,k'}e^{i\sqrt{\frac{1}{K}-2}\varphi(0)} + \text{H.c.})\right]\right\rangle = 2\sqrt{K}\sum_{k,k'}\text{Re}\{G'^{<}_{RL,k'k}(t,t)\},$$
$$\left\langle\left[\int\frac{dx}{2\pi}[\sqrt{1-2K}\nabla\varphi(x)], S_x\sum_{k,k'}(c'^{\dagger}_{cL,k}c'_{cR,k'}e^{i\sqrt{\frac{1}{K}-2}\varphi(0)} + \text{H.c.})\right]\right\rangle = \left(2\sqrt{K} - \frac{1}{\sqrt{K}}\right)\sum_{k,k'}\text{Re}\{G'^{<}_{RL,k'k}(t,t)\}, \tag{E5}$$

we obtain

$$I = \sqrt{K}\left(4 - \frac{1}{K}\right)\frac{e}{\hbar}\frac{J_{LR}}{\mathcal{L}}\sum_{k,k'}\text{Re}\{G'^{<}_{RL,k'k}(t,t)\}, \tag{E6}$$

where $G^{<}_{RL,k'k}(t,t') = i\langle c'^{\dagger}_{cL,k}(t')S_x(t)c'_{cR,k'}(t)e^{i\sqrt{\frac{1}{K}-2}\varphi(t)}\rangle$ is the lesser Green's function for $c_{cL/cR,k}$.

To evaluate the nonequilibrium current, we employ the equation of motion method to solve the lesser Green's function $G^{<}_{RL,k'k}(t-t')$,

$$\begin{aligned} i\frac{d}{dt'}G^{t}_{RL,k'k}(t-t') &= \left\langle T_t\left[S_x(t)c_{cR,k'}(t)e^{i\sqrt{\frac{1}{K}-2}\varphi(t)}\frac{d}{dt'}c^{\dagger}_{cL,k}(t')\right]\right\rangle \\ &= i\varepsilon_k\langle T_t[S_x(t)c_{cR,k'}(t)c^{\dagger}_{cL,k}(t')]\rangle \\ &\quad + i\frac{J_{LR}}{\mathcal{L}}\sum_{k''}\langle T_t[S_x(t)c_{cR,k'}(t)e^{i\sqrt{\frac{1}{K}-2}\varphi(t)}S_x(t') \\ &\quad \times c^{\dagger}_{cR,k''}(t')e^{-i\sqrt{\frac{1}{K}-2}\varphi(t')}]\rangle \\ &= -\varepsilon_k G^{t}_{RL,k'k}(t-t') - \frac{J_{LR}}{\mathcal{L}}\sum_{k''}G^{t}_{R,k'k''}(t-t'), \end{aligned} \tag{E7}$$

where $G^{t}_{R,k'k''}(t-t') = -i\langle T_t[S_x(t)c_{cR,k'}(t)e^{i\sqrt{\frac{1}{K}-2}\varphi(t)}S_x(t')$ $c^{\dagger}_{cR,k''}(t')e^{-i\sqrt{\frac{1}{K}-2}\varphi(t')}]\rangle$. We also define the noninteracting left lead time-ordered Green's function $g^{t}_{L,k}(t-t')$, which obeys the following equation,

$$\left(i\frac{d}{dt'} + \varepsilon_k\right)g^{t}_{L,k}(t-t') = -\delta(t-t'). \tag{E8}$$

Combing Eqs. (E7) and (E8), the time-ordered right-left Green's function $G^{t}_{RL,k'k}(t-t')$ can be expressed in terms of an integral equation as follows,

$$G^{t}_{RL,k'k}(t-t') = \frac{J_{LR}}{\mathcal{L}}\sum_{k''}\int dt_1 G^{t}_{R,k'k''}(t-t_1)g^{t}_{L,k}(t_1-t'), \tag{E9}$$

where the J_{LR} term gives the self-energy correction to either the left or right Green's functions. Note that we have already set $\hbar = 1$ for convenience and will put it back in the final form of the current. Assuming a uniform bias voltage $V_{L/R}$ is applied in the left/right lead with a finite jump in voltage at the dot, $V_L = V/2$ and $V_R = V/2$, the system is now in the nonequilibrium situation. Accordingly, we extend Eq. (S3) to the nonequilibrium case, which is expressed in terms of the contour-ordered Green's function $G^{c}_{RL,k'k}$. Equation (E9) has the same form in nonequilibrium except that the intermediate time integration runs on the counter c with τ_1 being the contour time,

$$G^{c}_{RL,k'k}(\tau,\tau') = \frac{J_{LR}}{\mathcal{L}}\sum_{k''}\int d\tau_1 G^{c}_{R,k'k''}(\tau,\tau_1)g^{c}_{L,k}(\tau_1,\tau'). \tag{E10}$$

In the weak tunneling limit, the J_{LR} is treated as a perturbation term in the Hamiltonian, we can expand the Green's function $G^{c}_{R,k'k''}(\tau,\tau_1)$ and keep the lowest order, which is $\langle S_x^2\rangle g^{c}_{R,k'k''}(\tau,\tau_1)b^{c}(\tau,\tau_1)$, where $g^{c}_{R,k'k''}(\tau,\tau_1)$ is the free-electron Green's function of the right lead, and $b^{c}(t-t') = \langle T_t[e^{i\sqrt{\frac{1}{K}-2}\varphi(t)}e^{-i\sqrt{\frac{1}{K}-2}\varphi(t')}]\rangle_0$ is the boson phase-phase correlator. Here, $\langle\cdots\rangle_0$ denotes that the expectation value is calculated only with respect to H'_b without the contribution from the J_{LR} term in the Hamiltonian where the boson field appearing as a phase, and $G^{c}_{RL,k'k}(\tau,\tau')$ now becomes

$$G^{c}_{RL,k'k}(\tau,\tau') = \frac{J_{LR}}{\mathcal{L}}\langle S_x^2\rangle\int d\tau_1 g^{c}_{R,k'}(\tau,\tau_1)b^{c}(\tau,\tau_1)g^{c}_{L,k}(\tau_1,\tau'). \tag{E11}$$

Since we are interested in the steady-state nonequilibrium transport, the transient behavior, which happens when the system initially turns to nonequilibrium, is neglected here. The time τ for the nonequilibrium case starts at $\tau = -\infty$, and follows the Keldysh contour from $\tau = -\infty$ to $\tau = +\infty$, and finally returns to $\tau = -\infty$. Applying the Keldysh contour, the lesser Green's function $G^<_{RL,k'k}(t-t')$ can be written as a real time integral and its analytical form is shown in Sec. IV A.

Because we are discussing the steady-state case, it is legitimate to set $t \to \infty$. Thus, we have $g^r_{R,k'}(t-t_1) + g^<_{R,k'}(t-t_1) = g^>_{R,k'}(t-t_1)$, $b^r(t-t_1) = b^>(t-t_1) - b^<(t-t_1)$. Since $b^<(\Delta t) = b^>(-\Delta t)$, we obtain $b^r(t-t_1) = b^<(t_1-t) - b^<(t-t_1)$. Furthermore, $G^<_{RL,k'k}(t-t')$ can be put into

$$\begin{aligned}G^<_{RL,k'k}(t-t') = \frac{J_{LR}}{\mathcal{L}}\langle S_x^2\rangle \int_{-\infty}^{\infty} dt_1 [g^r_{R,k'}(t-t_1) g^<_{L,k}(t_1-t') \\ + g^<_{R,k'}(t-t_1) g^a_{L,k}(t_1-t')] b^<(t-t_1) \\ + g^>_{R,k'}(t-t_1) g^<_{L,k}(t_1-t')[b^<(t_1-t) \\ - b^<(t-t_1)]. \end{aligned} \tag{E12}$$

The nonequilibrium current I now is given by

$$\begin{aligned} I = \sqrt{K}\left(4-\frac{1}{K}\right)\frac{e}{\hbar}\frac{J_{LR}^2}{\mathcal{L}^2}\langle S_x^2\rangle \sum_{k,k'} \iint \frac{d\omega d\omega'}{(2\pi)^2} \\ \times \mathrm{Re}\{[g^r_{R,k'}(\omega) g^<_{L,k}(\omega') + g^<_{R,k'}(\omega) g^a_{L,k}(\omega')] b^<(\omega'-\omega) \\ + g^>_{R,k'}(\omega) g^<_{L,k}(\omega')[b^<(\omega-\omega') - b^<(\omega'-\omega)]\}. \end{aligned} \tag{E13}$$

Since $b^<(\Delta t) = [b^<(-\Delta t)]^*$, $b^<(\omega)$ should be a real function. With the general relation between various types of Green's functions (g^r, g^a, $g^>$, $g^<$) held in any given system, $g^r - g^a = g^> - g^<$, we have the identity $\mathrm{Im}[g^r] = (g^> - g^<)/2$, so the current I takes the form

$$\begin{aligned} I = \sqrt{K}\left(4-\frac{1}{K}\right)\frac{e}{\hbar}\frac{J_{LR}^2}{\mathcal{L}^2}\langle S_x^2\rangle \sum_{k,k'} \iint \frac{d\omega d\omega'}{(2\pi)^2}[f(\omega'-\mu_L) \\ - f(\omega-\mu_R)]\mathrm{Im}[g^r_{R,k'}(\omega)]\mathrm{Im}[g^r_{L,k}(\omega')] b^<(\omega'-\omega). \end{aligned} \tag{E14}$$

Here, we have used the the following equalities, $g^<_{R/L,k'k''}(\omega) = -2if(\omega-\mu_{R/L})\mathrm{Im}[g^r_{R/L,k'k''}(\omega)]$, where $g^r_{R/L,k}(\omega) = [\omega - (\varepsilon_k - \mu_{R/L}) + i\eta]^{-1}$. In the thermodynamic limit $L \to \infty$, an explicit closed form of I can be obtained as

$$I = \sqrt{K}\left(4-\frac{1}{K}\right)\frac{e}{\hbar}\frac{J_{LR}^2}{(2\pi\hbar v_F)^2}\langle S_x^2\rangle \int_{-\infty}^{\infty}\int_{-\infty}^{\infty} d\varepsilon_k d\varepsilon_{k'}[f(\varepsilon_{k'}-eV/2) - f(\varepsilon_k + eV/2)]\int_{-\infty}^{\infty} dt\, b(t) e^{\frac{i}{\hbar}(\varepsilon_{k'}-\varepsilon_k)t}. \tag{E15}$$

Once we perform the integral over energy and time, we readily obtain the nonequilibrium current formula shown in Eq. (18).

If we go beyond the first-order perturbation, the second-order contribution to the Green's function $G^c_{RL,k'k}(\tau,\tau')$ is

$$\begin{aligned} G^{2c}_{RL,k'k}(\tau,\tau') = -i2\left(\frac{J_{LR}}{\mathcal{L}}\right)^2 \sum_{\substack{k'',k_1,k_2,\\k_3,k_4}} \int d\tau'' d\tau_1 d\tau_2 \Big\langle T_\tau\Big[S_x^2 c_{cR,k'}(\tau) e^{i\sqrt{\frac{1}{K}-2}\varphi(\tau)} c^\dagger_{cR,k_1}(\tau_1) c_{cL,k_2}(\tau_1) e^{-i\sqrt{\frac{1}{K}-2}\varphi(\tau_1)} \\ \times c^\dagger_{cL,k_3}(\tau_2) c_{cR,k_4}(\tau_2) e^{i\sqrt{\frac{1}{K}-2}\varphi(\tau_2)} c^\dagger_{cR,k''}(\tau'') e^{-i\sqrt{\frac{1}{K}-2}\varphi(\tau'')}\Big]\Big\rangle g^c_{L,k}(\tau_1,\tau'). \end{aligned} \tag{E16}$$

We examine one of the diagrams from the second-order perturbation term $G^{2c}_{RL,k'k}(\tau,\tau')$, which is

$$\Delta = -2\left(\frac{J_{LR}}{\mathcal{L}}\right)^2 \langle S_x^2\rangle \sum_{k_2,k_4}\int d\tau'' d\tau_1 d\tau_2 g^c_{R,k'}(\tau,\tau_1) B^c(\tau,\tau_1) g^c_{L,k_2}(\tau_1,\tau_2) g^c_{R,k_4}(\tau_2,\tau'') B^c(\tau_2,\tau'') g^c_{L,k}(\tau'',\tau'). \tag{E17}$$

If we choose the Keldysh contour, the contribution of Δ to the nonequilibrium current is proportional to $[j_{LR}^2(V/T)^{1/K-2}]^2$ at low temperatures. Actually, it is found that the contribution to the differential conductance from the nth-order perturbation term is proportional to $[j_{LR}^2(V/T)^{1/K-2}]^n$.

[1] A. C. Hewson, *The Kondo Problem to Heavy Fermions* (Cambridge University Press, Cambridge, UK, 1993).

[2] G. Baym and C. Pethick, *Landau Fermi-Liquid Theory: Concepts and Applications* (Wiley, Hoboken, NJ, 2007).

[3] H. V. Löhneysen, A. Rosch, M. Vojta, and P. Wölfle, Fermi-liquid instabilities at magnetic quantum phase transitions, Rev. Mod. Phys. **79**, 1015 (2007).

[4] C. Petrovic, P. G. Pagliuso, M. F. Hundley, R. Movshovich, J. L. Sarrao, J. D. Thompson, Z. Fisk, and P. Monthoux, Heavy-fermion superconductivity in $CeCoIn_5$ at 2.3 K, J. Phys.: Condens. Matter **13**, L337 (2001).

[5] L. Taillefer, Scattering and pairing in cuprate superconductors, Annu. Rev. Condens. Matter Phys. **1**, 51 (2010).

[6] D. C. Ralph and R. A. Buhrman, Observations of Kondo Scattering without Magnetic Impurities: A Point Contact Study of Two-Level Tunneling Systems in Metals, Phys. Rev. Lett. **69**, 2118 (1992).

[7] R. M. Potok, I. G. Rau, H. Shtrikman, Y. Oreg, and D. Goldhaber-Gordon, Observation of the two-channel Kondo effect, Nature (London) **446**, 167 (2007).

[8] S. Sachdev, *Quantum Phase Transitions*, 2nd ed. (Cambridge University Press, Cambridge, UK, 2011).

[9] E. Sela and I. Affleck, Nonequilibrium Transport through Double Quantum Dots: Exact Results near a Quantum Critical Point, Phys. Rev. Lett. **102**, 047201 (2009).

[10] G. Zhang, C. H. Chung, C. T. Ke, C. Y. Lin, H. Mebrahtu, A. I. Smirnov, G. Finkelstein, and H. U. Baranger, Universal nonequilibrium *I-V* curve at an interacting impurity quantum critical point, arXiv:1609.04765.

[11] C.-H. Chung, K. Le Hur, M. Vojta, and P. Wölfle, Nonequilibrium Transport at a Dissipative Quantum Phase Transition, Phys. Rev. Lett. **102**, 216803 (2009).

[12] C.-H. Chung, K. Le Hur, G. Finkelstein, M. Vojta, and P. Wölfle, Nonequilibrium quantum transport through a dissipative resonant level, Phys. Rev. B **87**, 245310 (2013).

[13] M. Heyl, A. Polkovnikov, and S. Kehrein, Dynamical Quantum Phase Transitions in the Transverse-Field Ising Model, Phys. Rev. Lett. **110**, 135704 (2013).

[14] D. Goldhaber-Gordon, H. Shtrikman, D. Mahalu, D. Abusch-Magder, U. Meirav, and M. A. Kastner, Kondo effect in a single-electron transistor, Nature (London) **391**, 156 (1998).

[15] H. T. Mebrahtu, I. V. Borzenets, D. E. Liu, H. Zheng, Y. V. Bomze, A. I. Smirnov, H. U. Baranger, and G. Finkelstein, Quantum phase transition in a resonant level coupled to interacting leads, Nature (London) **488**, 61 (2012).

[16] H. T. Mebrahtu, I. V. Borzenets, H. Zheng, Y. V. Bomze, A. I. Smirnov, S. Florens, H. U. Baranger, and G. Finkelstein, Observation of Majorana quantum critical behaviour in a resonant level coupled to a dissipative environment, Nat. Phys. **9**, 732 (2013).

[17] A. Mitra, S. Takei, Y. B. Kim, and A. J. Millis, Nonequilibrium Quantum Criticality in Open Electronic Systems, Phys. Rev. Lett. **97**, 236808 (2006).

[18] K. L. Hur, L. Henriet, A. Petrescu, K. Plekhanov, G. Roux, and M. Schiró, Many-body quantum electrodynamics networks: Non-equilibrium condensed matter physics with light, C. R. Phys. **17**, 808 (2016).

[19] M. A. Cazalilla and M.-C. Chung, Quantum quenches in the Luttinger model and its close relatives, J. Stat. Mech.: Theory Exp. (2016) 064004.

[20] N. Andrei, D. Iyer, and H. Guan, Quench dynamics in integrable systems, in *Strongly Interaction Quantum System out Equilibrium* (Oxford University Press, Oxford, UK, 2016).

[21] A. Mitra, Quantum quench dynamics, Annu. Rev. Condens. Matter Phys. **9**, 245 (2018).

[22] A. Y. Kitaev, Unpaired Majorana fermions in quantum wires, Phys. Usp. **44**, 131 (2001); R. M. Lutchyn, J. D. Sau, and S. Das Sarma, Majorana Fermions and a Topological Phase Transition in Semiconductor-Superconductor Heterostructures, Phys. Rev. Lett. **105**, 077001 (2010); Y. Oreg, G. Refael, and F. von Oppen, Helical Liquids and Majorana Bound States in Quantum Wires, *ibid.* **105**, 177002 (2010).

[23] S.-S. Yeh and J.-J. Lin, Two-channel Kondo effects in $Al/AlO_x/Sc$ planar tunnel junctions, Phys. Rev. B **79**, 012411 (2009).

[24] M. Fabrizio and A. O. Gogolin, Interacting one-dimensional electron gas with open boundaries, Phys. Rev. B **51**, 17827 (1995).

[25] E. H. Kim, Kondo effect in quantum dots coupled to Luttinger liquid leads, arXiv:cond-mat/0106575.

[26] A. Furusaki and N. Nagaosa, Kondo Effect in a Tomonaga-Luttinger Liquid, Phys. Rev. Lett. **72**, 892 (1994).

[27] S. Florens, P. Simon, S. Andergassen, and D. Feinberg, Interplay of electromagnetic noise and Kondo effect in quantum dots, Phys. Rev. B **75**, 155321 (2007).

[28] T. Giamarchi, *Quantum Physics in One Dimension* (Clarendon, Oxford, UK, 2004).

[29] A. Gogolin, A. Nersesyan, and A. Tsvelik, *Bosonization and Strongly Correlated Systems* (Cambridge University Press, Cambridge, UK, 2004).

[30] V. J. Emery and S. Kivelson, Mapping of the two-channel Kondo problem to a resonant-level model, Phys. Rev. B **46**, 10812 (1992).

[31] C.-H. Chung and S. Silotri, Quantum criticality in a Kondo quantum dot coupled to helical edge states of interacting 2D topological insulators, New J. Phys. **17**, 013005 (2015).

[32] A. Rosch, J. Kroha, and P. Wölfle, Kondo Effect in Quantum Dots at High Voltage: Universality and Scaling, Phys. Rev. Lett. **87**, 156802 (2001).

[33] H. Haug and A. Jauho, *Quantum Kinetics in Transport and Optics of Semiconductors* (Springer, Berlin, 2008).

[34] Y. Meir and N. S. Wingreen, Landauer Formula for the Current through an Interacting Electron Region, Phys. Rev. Lett. **68**, 2512 (1992).

[35] In deriving $G^{<}_{RL,k'k}(t-t')$ in Sec. IV A, we have used the identity $\langle c(t)e^{i\phi(t)}c(0)^{\dagger}e^{-i\phi(0)}\rangle = g(t)b(t)$ with $b(t) = \langle e^{i\phi(t)}e^{-i\phi(0)}\rangle_0 = ib^{>}(t)$, which separates the fermionic and bosonic correlation functions.

[36] A. Schiller and S. Hershfield, Toulouse limit for the nonequilibrium Kondo impurity: Currents, noise spectra, and magnetic properties, Phys. Rev. B **58**, 14978 (1998).

[37] C. J. Bolech and N. Shah, Consistent bosonization-debosonization. II. The two-lead Kondo problem and the fate of its nonequilibrium Toulouse point, Phys. Rev. B **93**, 085441 (2016).

[38] T. Larson, C. T. Ke, G. Zhang, E. Novais, H. Baranger, and G. Finkelstein (unpublished).

[39] K. T. Law, C. Y. Seng, P. A. Lee, and T. K. Ng, Quantum dot in a two-dimensional topological insulator: The two-channel Kondo fixed point, Phys. Rev. B **81**, 041305(R) (2010).